might induce severe liver damage [9-12] and pregnancy complications such as resorption and fetal growth restriction [13]. We also showed that these pregnancy complications can be suppressed by amino or carboxyl group surface modification [11,13].

The development of safe nanomaterials requires not only an evaluation of safety, but also the ability to predict their biological effects. Molecular biomarkers constitute an objective indicator for correlating against various physiological conditions or variation of disease state [14,15]. Biomarker studies have the potential to provide valuable information to identify early biological events associated with the adverse health effects of engineered nanomaterials in a development stage more easily and rapidly [16]. Studies of biomarkers for nanomaterials have barely advanced, but it is envisaged that a biomarker profile for exposure to nanomaterials would represent the unity of local and systemic physiological responses induced as a result of exposure. Therefore, there is a need to identify and evaluate biomarkers for nanomaterials that would be suitable for predicting the potential toxicity of nanomaterials as well as to facilitate the development of nanomaterials that are safe. In this regard, our previous study used sodium dodecyl sulfate-polyacrylamide gel electrophoresis (SDS-PAGE) analysis to show that the acute-phase proteins, haptoglobin, C-reactive protein, and serum amyloid A (SAA), can act as useful biomarkers for analyzing the risk of exposure to nanomaterials and their associated toxicity [17]. However, SDS-PAGE analysis has limited capacity for a comprehensive screen for biomarkers because it is based only on differences in molecular weight of proteins. Proteomics-based analyses such as two-dimensional (2D) gel separation and mass spectrometry are more suitable approaches for such a comprehensive study. Here, we performed a screen for biomarkers of nanomaterials using two-dimensional differential in gel electrophoresis (2D-DIGE), which is a gel-based approach like SDS-PAGE but separates proteins on the basis of their molecular weight and isoelectric point. We used this approach to identify hemopexin as a potential biomarker for predicting the biological effects induced by silica nanoparticles.

Methods

Materials

Silica particles were purchased from Micromod Partikeltechnologie (Rostock/Warnemünde, Germany). Silica particles with diameters of 70, 300, and 1,000 nm (nSP70, nSP300, and mSP1000, respectively) and nSP70 with surface carboxyl and amino groups (nSP70-C and nSP70-N, respectively), were used in this study. The silica particles were suspended in saline, sonicated for 5 min, and vortexed for 1 min prior to use.

Animals

Female BALB/c mice were purchased from Nippon SLC, Inc. (Shizuoka, Japan) and were used at 6 to 8 weeks of age. The mice were housed in a ventilated animal room maintained at 20 ± 2°C with a 12-h light/12-h dark cycle. The mice had free access to water and forage (FR-2, Funabashi farm, Chiba, Japan). All of the animal experimental procedures used in this study were performed in accordance with the Osaka University and National Institute of Biomedical Innovation guidelines for the welfare of animals.

2D-DIGE analysis

The BALB/c mice were treated intravenously with 0.8 mg/mouse nSP70 or saline. After 24 h, blood samples were collected, and plasma was harvested by centrifuging blood at 13,800×*g* for 15 min. ProteoPrep (Sigma-Aldrich, Saint Louis, MO, USA) was used to remove albumin and immunoglobulin from the plasma according to the manufacturer's instructions. Plasma proteins were purified from the plasma of the nSP70- or saline-treated mice using a 2D-Clean up Kit (GE Healthcare Biosciences, Piscataway, NJ, USA) and were labeled at the ratio of 50 μg proteins:400 pmol Cy3 or Cy5 protein-labeling dye (GE Healthcare Biosciences) in dimethylformamide according to the manufacturer's protocol. Briefly, 50 μg of each labeled sample was mixed with rehydration buffer (7 M urea, 2 M thiourea, 4% 3-(3-cholamidepropyl) dimethylammonio-1-propanesulphonate, 2% dithiothreitol, 2% Pharmalyte; GE Healthcare Biosciences) and applied to a 24-cm immobilized pH gradient gel strip (immobilized pH gradient (IPG) strip pH 4 to 7 NL) for separation in the first dimension. Samples for the spot picking gel were prepared without labeling by Cy dyes. For the second-dimension separation, the IPG strips were applied to SDS-PAGE gels (10% polyacrylamide and 2.7% *N,N'*-diallyltartardiamide gels). After electrophoresis, the gels were scanned with a laser fluoroimager (Typhoon Trio, GE Healthcare Biosciences). The spot picking gel was scanned after staining with Deep Purple Total Protein Stain (GE Healthcare Biosciences). Quantitative analysis of protein spots was carried out with Decyder-DIA software (GE Healthcare Biosciences). Protein spots representing greater than twofold alteration in expression were picked using an Ettan Spot Picker (GE Healthcare Biosciences).

In-gel tryptic digestion

The gel pieces were destained with 50% acetonitrile (ACN)/25 mM NH_4HCO_3 for 10 min, dehydrated with 100% ACN for 10 min, and then dried using a centrifugal concentrator (TOMY SEIKO, Tokyo, Japan). Next, 8 μl of 20 μl/ml trypsin solution (Promega, Madison, WI, USA) diluted fivefold in 50 mM NH_4HCO_3 was

added to each gel piece, which was then incubated overnight at 37°C. We used three solutions to extract the resulting peptide mixtures from the gel pieces. First, 50 μl of 50% (*v*/*v*) ACN in 0.1% aqueous trifluoroacetic acid (TFA) was added to the gel pieces, which were then sonicated for 30 min. Next, we collected the solution and added 80% (*v*/*v*) ACN in 0.1% TFA. Finally, 100% ACN was added for the last extraction. The peptide solutions were dried and resuspended in 10 μl of 0.1% formic acid. The resulting peptide mixture was then analyzed by nano-flow liquid chromatography/tandem mass spectrometry (maXis, Bruker Daltonik GmbH, Bremen, Germany). The Mascot search engine (Matrix Science Inc., Boston, MA, USA) was initially used to query the entire theoretical tryptic peptide as well as the Swiss-Prot protein sequence database.

Measurement of hemopexin

The BALB/c mice were treated intravenously with 0.8 mg/mouse of the silica particles nSP70, nSP300, mSP1000, nSP70-C, and nSP70-N or with saline. Blood samples were collected at 2, 6, 24, 48, and 72 h after treatment. For assessment of the sensitivity of hemopexin levels to the concentration of silica particles, the BALB/c mice were treated intravenously with 0.05, 0.2, or 0.8 mg/mouse nSP70. After 24 h, blood samples were collected, and plasma was harvested by centrifuging blood at 13,800×*g* for 15 min. Plasma levels of hemopexin were measured using a commercial enzyme-linked immunosorbent assay (ELISA) kit (Life Diagnostics, West Chester, PA, USA), according to the manufacturer's instructions.

Plasma biochemistry

The BALB/c mice were treated intravenously with 0.8 mg/mouse nSP70 or saline. After 2, 6, 24, and 48 h, blood samples were collected, and plasma was harvested by centrifuging blood at 13,800×*g* for 15 min. Total hemoglobin and heme in the blood of the nSP70-treated mice were determined by BioAssay Systems QuantiChrom™ Assay Kits (BioAssay Systems, Hayward, CA, USA). Also, plasma levels of total bilirubin (TBIL) and direct bilirubin (DBIL) were measured by a biochemical auto analyzer, FUJI DRI-CHEM 7000 (Fujifilm, Tokyo, Japan), and the level of indirect bilirubin was calculated from these values.

Statistical analysis

All results are expressed as means ± standard error of the mean (SEM). Statistical comparisons between groups were performed by one-way analysis of variance (ANOVA) with the Bonferroni test.

Results

Characteristics of silica particles

Silica particles are well suited for studying the influence of nanomaterial size on biodistribution and various biological effects because they show much better dispersibility in aqueous solutions than most other nanomaterials [18]. We used three different-sized silica particles with diameters between 70 and 1,000 nm (nSP70, nSP300, and mSP1000) and nSP70 with carboxyl (nSP70-C) and amino (nSP70-N) surface functional groups. As we have described previously [9,10,13], all silica nanoparticles were confirmed by transmission electron microscopy to be smooth-surfaced spheres. The hydrodynamic diameters of nSP70, nSP300, and mSP1000 were 65, 322, and 1,140 nm, respectively, and their zeta potentials or overall surface potentials were −53, −62, and −67 mV, respectively. For nSP70-C and nSP70-N, the hydrodynamic diameters were 70 and 72 nm, respectively, and their zeta potentials were −76 and −29 mV, respectively. These results indicate that the carboxyl and amino surface modifications altered the surface charge of the particles. The size distribution spectrum of each set of silica particles showed a single peak, and the measured hydrodynamic diameter corresponded almost precisely to the primary particle size of each set of silica particles. These results indicate that the silica particles used in this study were well dispersed in solution.

2D-DIGE analysis and identification of differentially expressed proteins

To identify protein biomarkers of nanomaterials in mice, we analyzed changes in the levels of plasma proteins following treatment with nSP70 by using 2D-DIGE. Plasma proteins isolated after treatment with saline or 0.8 mg/mouse nSP70 were labeled with Cy3 and Cy5, respectively, and were used for 2D-DIGE analysis. The reason why we chose the dose of silica particles for treatment is that none of the silica particles induced any significant changes in the levels of aspartate aminotransferase (AST), alanine aminotransferase (ALT), and blood urea nitrogen and that all parameters remained within the physiological range, as we have previously reported [17]. Quantitative image analysis revealed 59 spots showing increased protein levels and 23 spots showing decreased protein levels in the plasma of nSP70-treated mice compared with controls. We selected a total of eight candidate spots showing the highest increases and decreases in protein expression levels. Then, liquid chromatography/time-of-flight/mass spectrometry (LC/TOF/MS) analysis of the spots subsequently identified seven different proteins (Figure 1). Among these proteins, haptoglobin, hemopexin, and alpha-1-acid glycoprotein 1, which are acute-phase proteins, displayed increased expression in the plasma of nSP70-treated mice. Four proteins, including inter-alpha-trypsin inhibitor, complement C4-B,

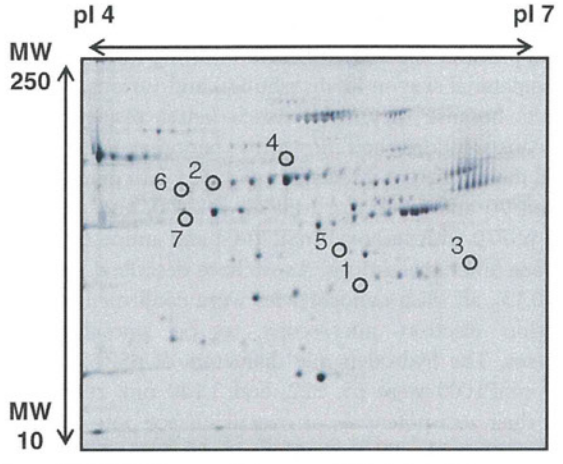

Figure 1 2D-DIGE image of fluorescent-labeled proteins. Proteins from the plasma after treatment with saline or nSP70 were labeled with Cy3 and Cy5, respectively, and used for performing 2D electrophoresis.

Cullin-4A, and serotransferrin, displayed decreased expression in the plasma of nSP70-treated mice (Table 1). These findings are consistent with the results of our previous study identifying haptoglobin, showing the highest level in this study, as a candidate biomarker using SDS-PAGE analysis. We selected a candidate biomarker from among the proteins which displayed increased expression at first. However, in the future, there is a need to identify various biomarkers by evaluating candidate proteins which displayed not only increased expression but also decreased expression to improve the accuracy for predicting the biological effects induced by nanomaterials. Here, we focused on hemopexin, which showed the second highest expression level among the identified candidate biomarkers after haptoglobin.

Plasma hemopexin levels after treatment with silica particles

Hemopexin is known as an acute-phase protein, mainly synthesized in the liver [19]. To assess the potential of hemopexin as a biomarker, we examined whether there were time-dependent changes in the plasma levels of hemopexin levels after treatment with different-sized silica particles. The BALB/c mice were treated intravenously with 0.8 mg/mouse nSP70, nSP300, or mSP1000. After 6, 24, or 72 h, we examined the plasma levels of hemopexin by ELISA. We observed no changes in the plasma levels of hemopexin in mice treated with nSP300 or mSP1000 over the time course of the experiment. However, mice treated with nSP70 showed an increase in plasma levels of hemopexin at 24 h after treatment, and the plasma level of hemopexin in nSP70-treated mice remained significantly higher than that of controls at 72 h after treatment (Figure 2A). These results indicate that the smaller the particle size, the greater the increase in plasma levels of hemopexin induced by silica particles. We then assessed the sensitivity of hemopexin induction to lower concentrations of silica particles. The BALB/c mice were treated intravenously with 0.05, 0.2, or 0.8 mg/mouse nSP70. After 24 h, we examined the plasma levels of hemopexin by ELISA and found that the plasma level of hemopexin increased in a dose-dependent manner (Figure 2B). These results indicate that the level of induction of hemopexin is dependent on the concentration of silica particles. Taken together, these findings highlight the potential of hemopexin as a valuable biomarker for analyzing the risk and toxicity of exposure to silica nanoparticles. Now, to evaluate the sensitivity of hemopexin to serve as a biomarker of a more realistic exposure, we have assessed the response of hemopexin to silica nanoparticles introduced via different routes.

Hemolytic activity of silica nanoparticles

Hemopexin is a heme-binding plasma glycoprotein that forms the second line of defense against hemoglobin-mediated oxidative damage during intravascular hemolysis [20]. Intravascular hemolysis causes the release of massive amounts of hemoglobin and heme into the plasma, where they are rapidly bound by haptoglobin and hemopexin, respectively [21]. Because nSP70 induced an increase in the plasma levels of haptoglobin and hemopexin in mice, we investigated the possibility

Table 1 Identification of candidate proteins as biomarkers

Spot	Protein name	Accession number	MW (kD)	pI	Expression ratio (nSP70/saline) (fold)
1	Haptoglobin	[Swiss-Prot:Q61646]	38.75	5.88	375.44
2	Hemopexin	[Swiss-Prot:Q91X72]	51.34	7.92	3.25
3	Alpha-1-acid glycoprotein 1	[Swiss-Prot:Q60590]	23.89	5.58	3.05
4	Inter-alpha-trypsin inhibitor	[Swiss-Prot:Q61703]	105.93	6.82	0.40
5	Complement C4-B	[Swiss-Prot:P01029]	192.89	7.38	0.39
6	Cullin-4A	[Swiss-Prot:Q3TCH7]	87.75	8.53	0.37
7	Serotransferrin	[Swiss-Prot:Q921I1]	76.72	6.94	0.30

The differentially expressed spots were identified by LC/TOF/MS. pI, isoelectric point.

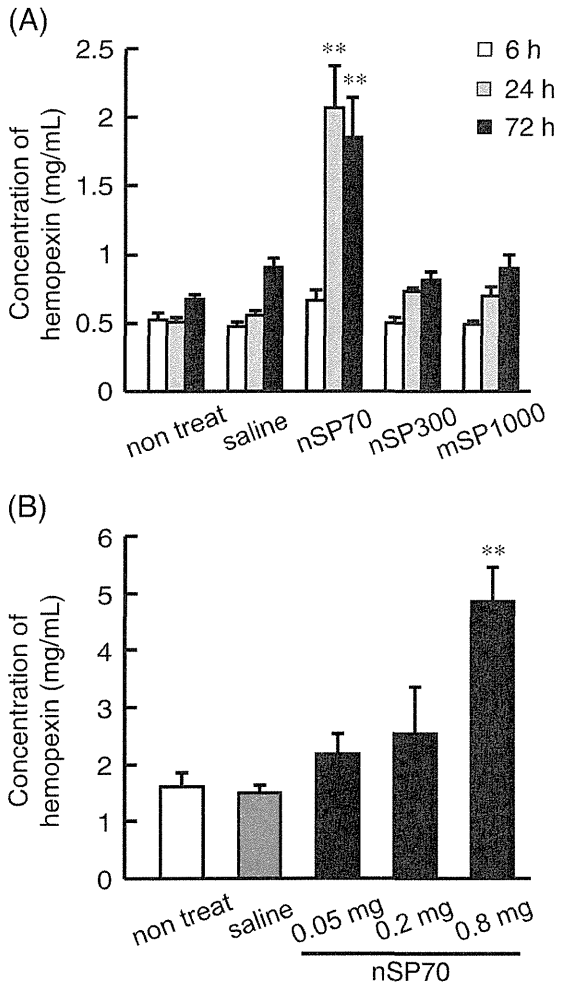

Figure 2 Plasma levels of hemopexin after treatment with silica particles. BALB/c mice were treated intravenously with 0.8 mg/mouse nSP70, nSP300, or mSP1000. (**A**) After 6, 24, and 72 h, the plasma levels of hemopexin in the mice were determined by ELISA. (**B**) BALB/c mice were treated intravenously with 0.05, 0.2, or 0.8 mg/mouse nSP70. After 24 h, blood samples were collected. The plasma levels of hemopexin in treated mice were determined by ELISA. Data are presented as mean ± SEM ($n = 5$; Double asterisks denote $P < 0.01$ versus the value for saline-treated group by ANOVA).

that silica nanoparticles could induce hemolytic activity. We assessed plasma levels of heme and hemoglobin 2, 6, 24, or 48 h after treatment of the BALB/c mice intravenously with 0.8 mg/mouse of nSP70. At this dose, nSP70 did not induce any significant increases in the plasma levels of heme (Figure 3A) or hemoglobin (Figure 3B) at all time points.

During hemolysis, hemoglobin is released into the plasma from damaged red blood cells and leads to an increase in plasma levels of indirect bilirubin [22-24]. Thus, although nSP70 did not induce a significant increase in the plasma levels of heme or hemoglobin, we investigated whether nSP70 induced hemolytic activity that resulted in an increased plasma level of indirect bilirubin. Following treatment of mice with nSP70, we measured plasma levels of TBIL and DBIL and calculated the level of indirect bilirubin from these values. We found no changes in the plasma levels of TBIL (Figure 3C), DBIL (Figure 3D), or indirect bilirubin (Figure 3E) over the time course of the experiment. Taken together, these results clearly show that nSP70 does not induce hemolytic activity in mice under these conditions.

Surface modification of nSP70

Previously, we demonstrated that surface properties of silica nanoparticles play an important role in determining their safety [11,13]. For instance, our group showed that surface modification of nSP70 with amine or carboxyl groups altered the intracellular distribution of the nanoparticles, had an effect on cell proliferation [11], and suppressed toxic biological effects of silica particles such as inflammatory responses. To assess whether hemopexin could predict the strength of toxicity induced by silica nanoparticles, we examined the plasma levels of hemopexin in the mice after administration of nSP70 with amino or carboxyl group surface modifications. The BALB/c mice were treated intravenously with 0.8 mg/mouse of nSP70, nSP70-C, or nSP70-N. After 2, 6, 24, or 48 h, we examined the plasma levels of hemopexin by ELISA. The mice treated with nSP70, nSP70-C, and nSP70-N did not show any elevated level of hemopexin at 2 or 6 h. At 24 h, the plasma level of hemopexin in mice treated with nSP70-N was significantly lower than that in mice treated with unmodified nSP70. On the other hand, the plasma level of hemopexin in mice treated with nSP70-C was similar to that in nSP70-treated mice and significantly higher than that in saline-treated mice (Figure 4A). At the same time, the plasma levels of haptoglobin (Figure 4B) and SAA (Figure 4C) in mice treated with nSP70-C were significantly lower than those in nSP70-treated mice, which is consistent with our previously reported results [17]. These results indicate that there are differences in the mechanisms underlying the production of hemopexin and other acute-phase proteins induced by nSP70-C.

Discussion

By using biomarkers, we are able to predict not only the present disease and clinical condition, but also the risk of acquiring disease in the future. Therefore, it is necessary to progress studies of biomarkers for nanomaterials because very little information is available on the biological effects of nanomaterials. Here, we used 2D-DIGE analysis to perform a comprehensive screen of plasma

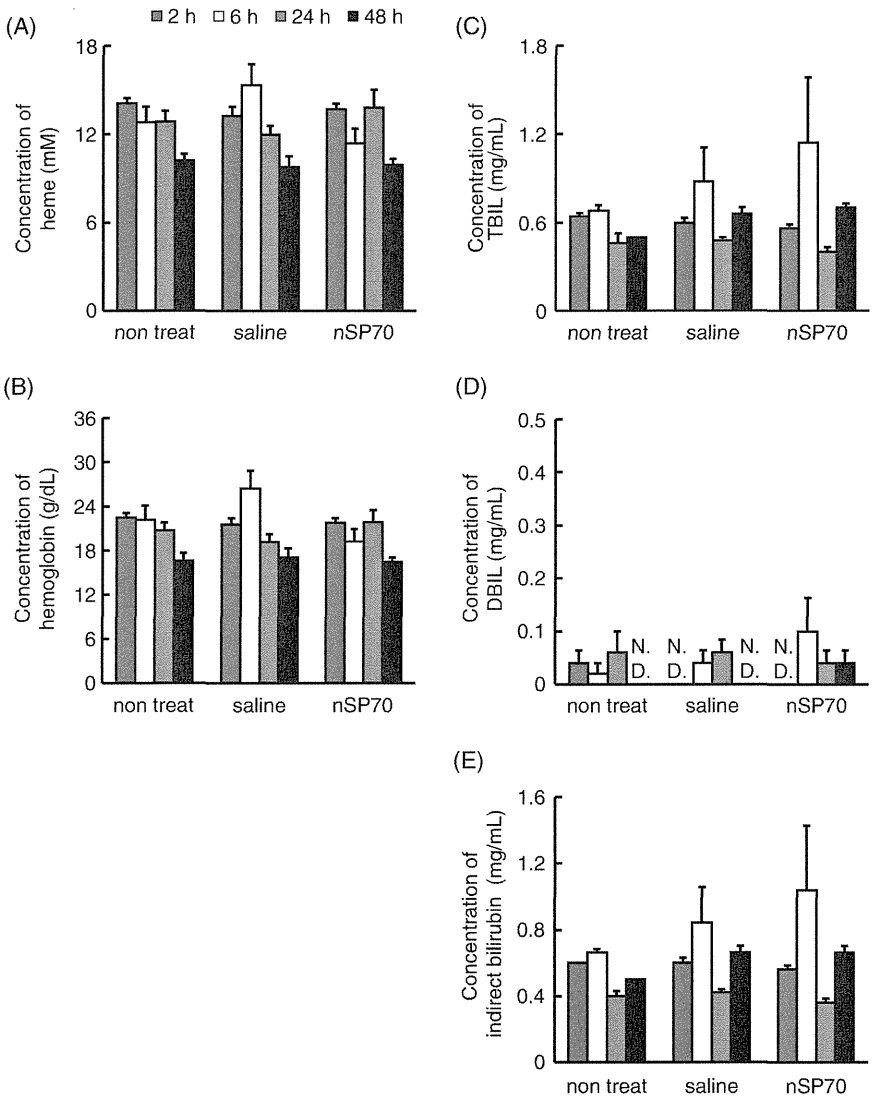

Figure 3 Hemolytic activity of silica nanoparticles. BALB/c mice were treated intravenously with 0.8 mg/mouse nSP70. After 2, 6, 24, and 48 h, we examined the level of (**A**) total heme and (**B**) hemoglobin in the blood of treated mice. The levels of (**C**) TBIL and (**D**) DBIL were measured, and (**E**) the level of indirect bilirubin was calculated from these values.

proteins to identify protein biomarkers of nanomaterials. We identified hemopexin (Table 1) as a useful biomarker for analyzing the biological responses associated with exposure to silica nanoparticles. Because 2D-DIGE is a proteomic method, this approach has potential to uncover the as yet unknown biological effects of nanomaterials.

On the other hand, an inherent disadvantage of 2D electrophoresis is the poor resolution of hydrophobic proteins [25,26]. Hence, it is likely that integral membrane proteins are strongly underrepresented. Isobaric tags for relative and absolute quantification or iTRAQ is a comprehensive gel-free quantitative proteomic method based on mass spectrometry [27,28]. This approach can be used to generate proteomic profiles that reflect the pathological state of organs and aid in the early detection of diseases [29,30]. We envisage that a combination of comprehensive proteomic methods would help to identify potential toxicities of nanomaterials during their development and contribute to the establishment of strategies to ensure their safety.

Silica materials with amorphous particle morphology are known to cause the hemolysis of mammalian red blood cells [31,32]. For this reason, we investigated the possibility that silica nanoparticles could induce hemolytic activity. While the exact mechanism is still

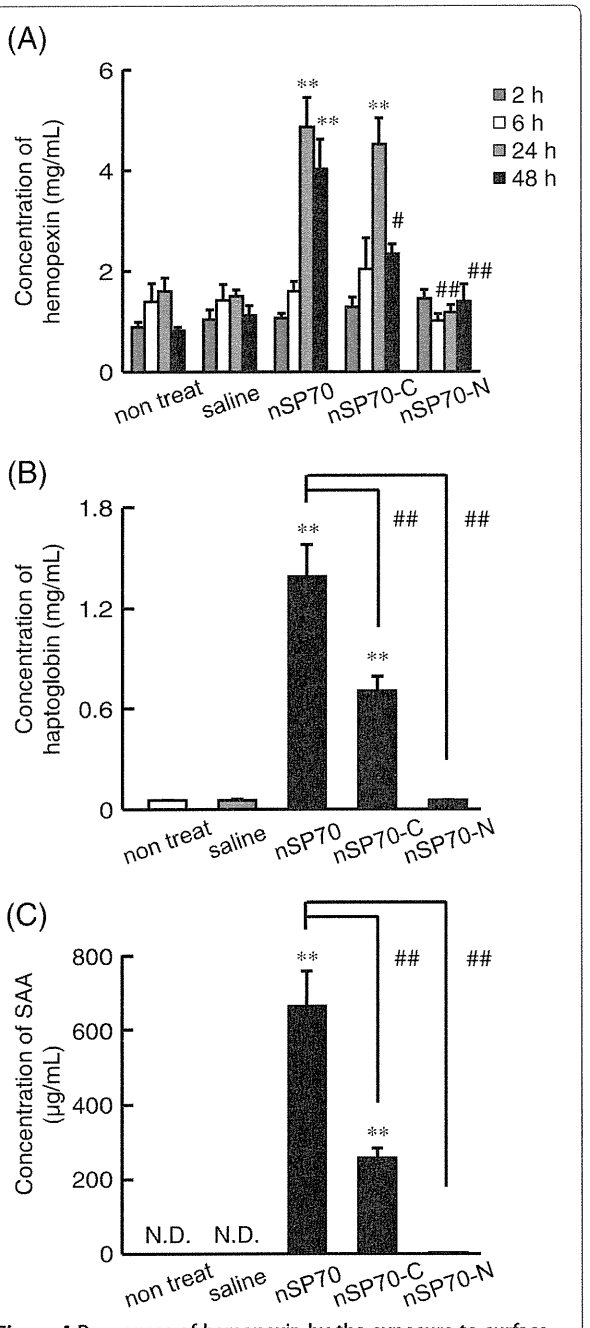

Figure 4 Responses of hemopexin by the exposure to surface modified nSP70. BALB/c mice were treated intravenously with nSP70 modified with amino (nSP70-N) or carboxyl (nSP70-C) groups at 0.8 mg/mouse. (**A**) After 2, 6, 24, and 48 h, the levels of hemopexin in the plasma of treated mice were examined by ELISA. The plasma levels of (**B**) haptoglobin and (**C**) SAA were determined by ELISA after 24 h. Data are presented as mean ± SEM. ($n = 5$; Double asterisks denote $P < 0.01$ versus the value for the saline-treated group by ANOVA, single hash denotes $P < 0.05$, and double hash denote $P < 0.01$ versus the value for the nSP70-treated group by ANOVA).

under investigation, most reports agree that the hemolytic activity of silica particles is related to surface characteristics such as area and curvature [33-35]. However, we found that nSP70 at 0.8 mg/mouse does not induce hemolytic activity through elevation of haptoglobin and hemopexin (Figure 3). We are continuing investigations to understand the biological mechanisms associated with the elevation of hemopexin after exposure to silica nanoparticles.

We then examined the effects of surface modification of silica nanoparticles on the production of hemopexin. Compared to controls, hemopexin was not induced by nSP70-N but was induced to a significantly higher level by nSP70-C, which was a similar level to that induced by unmodified nSP70 (Figure 4A). On the other hand, the plasma levels of haptoglobin (Figure 4B) and SAA (Figure 4C) in mice treated with nSP70-C were significantly lower than those in mice treated with nSP70, as reported previously [17]. These results suggest that the production of acute-phase proteins depends on the characteristics of the nanomaterials and that nSP70-C induces some biological effects associated with the elevation of hemopexin. Increased hemopexin levels have been found in patients with diabetes mellitus and are associated with some malignancies, such as malignant melanoma and breast cancer [20,36,37]. Elevated hemopexin levels have also been found in inflammatory psychiatric disorders, such as major depression, schizophrenia, and mania [38]. Taken together, these findings suggest that hemopexin might be associated with these diseases so it is possible that the induced elevation of hemopexin by both nSP70 and nSP70-C is related to the induction of inflammatory responses. Therefore, we are currently analyzing not only the mechanisms underlying the differences in production of hemopexin, haptoglobin, and SAA induced by nSP70-C and nSP70, but also the relationship. It could be speculated that there are differences between the fates of the injected nSP70 and nSP70-C. Therefore, there is a need to evaluate the distribution or accumulation of the injected nanoparticles in the liver where acute-phase proteins are known to be produced. An understanding of these mechanisms will advance the use of biomarkers for different purposes and improve the predictive value of these biomarkers.

Hemopexin is one of the acute-phase proteins released from the liver, and its production is known to be regulated by cytokines. For instance, interleukin (IL)-6 and IL-22 induce the hepatic production of circulating SAA [39,40]. Furthermore, it is conceivable that instead of inflammatory cytokines, small silica particles act directly on the liver to induce the release of acute-phase proteins. However, nSP70, at this dose, did not induce any significant elevation of liver injury or dysfunction

markers, such as ALT or AST. Therefore, it is unclear why nanomaterials induce the production of acute-phase proteins. We are currently analyzing the detailed mechanism by which silica particles induce acute-phase proteins.

Conclusions

We demonstrated that 2D-DIGE analysis is a useful approach for identifying novel biomarkers of nanomaterials. Using this approach, we identified hemopexin as a useful biomarker and showed here that hemopexin can act as a useful biomarker for analyzing the biological responses associated with exposure to silica nanoparticles. We believe that this study will contribute to the development of biomarkers for ensuring the safety of silica nanoparticles.

Abbreviations

2D: Two-dimensional; 2D-DIGE: Two-dimensional differential in gel electrophoresis; ACN: Acetonitrile; ALT: Alanine amino transferase; AST: Aspartate amino transferase; DBIL: Direct bilirubin; ELISA: Enzyme-linked immunosorbent assay; IL: Interleukin; IPG: Immobilized pH gradient; iTRAQ: Isobaric tags for relative and absolute quantification; LC/TOF/MS: Liquid chromatography/time-of-flight/mass spectrometry; SAA: Serum amyloid A; SDS-PAGE: Sodium dodecyl sulfate-polyacrylamide gel electrophoresis; TBIL: Total bilirubin; TFA: Trifluoroacetic acid.

Competing interests

The authors declare that they have no competing interests.

Authors' contributions

KH and YY designed the study. KH, KY, YM, HP, TO, TN, and AK performed the experiments. KH and YY collected and analyzed the data. KH and YY wrote the manuscript. KN, YA, HK, ST, HN, and TY gave technical support and conceptual advice. YT supervised all of the projects. All authors discussed the results and commented on the manuscript. All authors read and approved the final manuscript.

Acknowledgments

This study was supported in part by Grants-in-Aid for Scientific Research from the Ministry of Education, Culture, Sports, Science and Technology of Japan and from the Japan Society for the Promotion of Science (JSPS). This study was also supported in part by the following: Health Labour Sciences Research Grants from the Ministry of Health, Labor and Welfare of Japan; Health Sciences Research Grants for Research on Publicly Essential Drugs and Medical Devices from the Japan Health Sciences Foundation; the Global Environment Research Fund from the Minister of the Environment; the Knowledge Cluster Initiative; The Nagai Foundation Tokyo; the Cosmetology Research Foundation; the Smoking Research Foundation; the Research Foundation for Pharmaceutical Sciences; and The Japan Food Chemical Research Foundation.

Author details

[1]Laboratory of Toxicology and Safety Science, Graduate School of Pharmaceutical Sciences, Osaka University, 1-6 Yamadaoka, Suita, Osaka 565-0871, Japan. [2]Laboratory of Biopharmaceutical Research, National Institute of Biomedical Innovation, 7-6-8, Saito-Asagi, Ibaraki, Osaka 567-0085, Japan. [3]Cancer Biology Research Center, Sanford Research/USD, 2301 E. 60th Street N, Sioux Falls, SD 57104, USA. [4]The Center for Advanced Medical Engineering and Informatics, Osaka University, 1-6, Yamadaoka, Suita, Osaka 565-0871, Japan. [5]Division of Foods, National Institute of Health Sciences, 1-18-1 Kamiyoga, Setagaya-ku, Tokyo 158-8501, Japan.

Received: 16 July 2012 Accepted: 21 September 2012
Published: 8 October 2012

References

1. Augustin MA, Sanguansri P: **Nanostructured materials in the food industry.** *Adv Food Nutr Res* 2009, **58**:183–213.
2. Bowman DM, van Calster G, Friedrichs S: **Nanomaterials and regulation of cosmetics.** *Nat Nanotechnol* 2010, **5**:92.
3. Kagan VE, Bayir H, Shvedova AA: **Nanomedicine and nanotoxicology: two sides of the same coin.** *Nanomedicine* 2005, **1**:313–316.
4. Nel A, Xia T, Madler L, Li N: **Toxic potential of materials at the nanolevel.** *Science* 2006, **311**:622–627.
5. Merget R, Bauer T, Kupper HU, Philippou S, Bauer HD, Breitstadt R, Bruening T: **Health hazards due to the inhalation of amorphous silica.** *Arch Toxicol* 2002, **75**:625–634.
6. Knopp D, Tang D, Niessner R: **Review: bioanalytical applications of biomolecule-functionalized nanometer-sized doped silica particles.** *Anal Chim Acta* 2009, **647**:14–30.
7. Napierska D, Thomassen LC, Lison D, Martens JA, Hoet PH: **The nanosilica hazard: another variable entity.** *Part Fibre Toxicol* 2010, **7**:39.
8. Lankoff A, Arabski M, Wegierek-Ciuk A, Kruszewski M, Lisowska H, Banasik-Nowak A, Rozga-Wijas K, Wojewodzka M, Slomkowski S: **Effect of surface modification of silica nanoparticles on toxicity and cellular uptake by human peripheral blood lymphocytes in vitro.** *Nanotoxicology* 2012. doi:10.3109/17435390.2011.649796.
9. Nabeshi H, Yoshikawa T, Matsuyama K, Nakazato Y, Matsuo K, Arimori A, Isobe M, Tochigi S, Kondoh S, Hirai T, Akase T, Yamashita T, Yamashita K, Yoshida T, Nagano K, Abe Y, Yoshioka Y, Kamada H, Imazawa T, Itoh N, Nakagawa S, Mayumi T, Tsunoda S, Tsutsumi Y: **Systemic distribution, nuclear entry and cytotoxicity of amorphous nanosilica following topical application.** *Biomaterials* 2011, **32**:2713–2724.
10. Nabeshi H, Yoshikawa T, Matsuyama K, Nakazato Y, Tochigi S, Kondoh S, Hirai T, Akase T, Nagano K, Abe Y, Yoshioka Y, Kamada H, Itoh N, Tsunoda S, Tsutsumi Y: **Amorphous nanosilica induce endocytosis-dependent ROS generation and DNA damage in human keratinocytes.** *Part Fibre Toxicol* 2011, **8**:1.
11. Nabeshi H, Yoshikawa T, Arimori A, Yoshida T, Tochigi S, Hirai T, Akase T, Nagano K, Abe Y, Kamada H, Tsunoda S, Itoh N, Yoshioka Y, Tsutsumi Y: **Effect of surface properties of silica nanoparticles on their cytotoxicity and cellular distribution in murine macrophages.** *Nanoscale Res Lett* 2011, **6**:93.
12. Nabeshi H, Yoshikawa T, Matsuyama K, Nakazato Y, Arimori A, Isobe M, Tochigi S, Kondoh S, Hirai T, Akase T, Yamashita T, Yamashita K, Yoshida T, Nagano K, Abe Y, Yoshioka Y, Kamada H, Imazawa T, Itoh N, Kondoh M, Yagi K, Mayumi T, Tsunoda S, Tsutsumi Y: **Amorphous nanosilicas induce consumptive coagulopathy after systemic exposure.** *Nanotechnology* 2012, **23**:045101.
13. Yamashita K, Yoshioka Y, Higashisaka K, Mimura K, Morishita Y, Nozaki M, Yoshida T, Ogura T, Nabeshi H, Nagano K, Abe Y, Kamada H, Monobe Y, Imazawa T, Aoshima H, Shishido K, Kawai Y, Mayumi T, Tsunoda S, Itoh N, Yoshikawa T, Yanagihara I, Saito S, Tsutsumi Y: **Silica and titanium dioxide nanoparticles cause pregnancy complications in mice.** *Nat Nanotechnol* 2011, **6**:321–328.
14. Casado B, Iadarola P, Luisetti M, Kussmann M: **Proteomics-based diagnosis of chronic obstructive pulmonary disease: the hunt for new markers.** *Expert Rev Proteomics* 2008, **5**:693–704.
15. Ferte C, Andre F, Soria JC: **Molecular circuits of solid tumors: prognostic and predictive tools for bedside use.** *Nat Rev Clin Oncol* 2010, **7**:367–380.
16. Li N, Nel AE: **Feasibility of biomarker studies for engineered nanoparticles: what can be learned from air pollution research.** *J Occup Environ Med* 2011, **53**:S74–79.
17. Higashisaka K, Yoshioka Y, Yamashita K, Morishita Y, Fujimura M, Nabeshi H, Nagano K, Abe Y, Kamada H, Tsunoda S, Yoshikawa T, Itoh N, Tsutsumi Y: **Acute phase proteins as biomarkers for predicting the exposure and toxicity of nanomaterials.** *Biomaterials* 2011, **32**:3–9.
18. He X, Nie H, Wang K, Tan W, Wu X, Zhang P: **In vivo study of biodistribution and urinary excretion of surface-modified silica nanoparticles.** *Anal Chem* 2008, **80**:9597–9603.
19. Tolosano E, Altruda F: **Hemopexin: structure, function, and regulation.** *DNA Cell Biol* 2002, **21**:297–306.
20. Delanghe JR, Langlois MR: **Hemopexin: a review of biological aspects and the role in laboratory medicine.** *Clin Chim Acta* 2001, **312**:13–23.

21. Vinchi F, Gastaldi S, Silengo L, Altruda F, Tolosano E: **Hemopexin prevents endothelial damage and liver congestion in a mouse model of heme overload.** *Am J Pathol* 2008, **173**:289–299.
22. Lagan AL, Melley DD, Evans TW, Quinlan GJ: **Pathogenesis of the systemic inflammatory syndrome and acute lung injury: role of iron mobilization and decompartmentalization.** *Am J Physiol Lung Cell Mol Physiol* 2008, **294**:L161–174.
23. Nielsen MJ, Moestrup SK: **Receptor targeting of hemoglobin mediated by the haptoglobins: roles beyond heme scavenging.** *Blood* 2009, **114**:764–771.
24. Nielsen MJ, Moller HJ, Moestrup SK: **Hemoglobin and heme scavenger receptors.** *Antioxid Redox Signal* 2010, **12**:261–273.
25. Lopez JL: **Two-dimensional electrophoresis in proteome expression analysis.** *J Chromatogr B Analyt Technol Biomed Life Sci* 2007, **849**:190–202.
26. Sa-Correia I, Teixeira MC: **2D electrophoresis-based expression proteomics: a microbiologist's perspective.** *Expert Rev Proteomics* 2010, **7**:943–953.
27. Aggarwal K, Choe LH, Lee KH: **Shotgun proteomics using the iTRAQ isobaric tags.** *Brief Funct Genomic Proteomic* 2006, **5**:112–120.
28. Treumann A, Thiede B: **Isobaric protein and peptide quantification: perspectives and issues.** *Expert Rev Proteomics* 2010, **7**:647–653.
29. Xu J, Khor KA, Sui J, Zhang J, Tan TL, Chen WN: **Comparative proteomics profile of osteoblasts cultured on dissimilar hydroxyapatite biomaterials: an iTRAQ-coupled 2-D LC-MS/MS analysis.** *Proteomics* 2008, **8**:4249–4258.
30. Yang X, Yang S, Wang J, Zhang X, Wang C, Hong G: **Expressive proteomics profile changes of injured human brain cortex due to acute brain trauma.** *Brain Inj* 2009, **23**:830–840.
31. Gerashchenko BI, Gun'ko VM, Gerashchenko II, Mironyuk IF, Leboda R, Hosoya H: **Probing the silica surfaces by red blood cells.** *Cytometry* 2002, **49**:56–61.
32. Murashov V, Harper M, Demchuk E: **Impact of silanol surface density on the toxicity of silica aerosols measured by erythrocyte haemolysis.** *J Occup Environ Hyg* 2006, **3**:718–723.
33. Slowing II, Wu CW, Vivero-Escoto JL, Lin VS: **Mesoporous silica nanoparticles for reducing hemolytic activity towards mammalian red blood cells.** *Small* 2009, **5**:57–62.
34. Lin YS, Haynes CL: **Impacts of mesoporous silica nanoparticle size, pore ordering, and pore integrity on hemolytic activity.** *J Am Chem Soc* 2010, **132**:4834–4842.
35. Yu T, Malugin A, Ghandehari H: **Impact of silica nanoparticle design on cellular toxicity and hemolytic activity.** *ACS Nano* 2011, **5**:5717–5728.
36. Manuel Y, Defontaine MC, Bourgoin JJ, Dargent M, Sonneck JM: **Serum haemopexin levels in patients with malignant melanoma.** *Clin Chim Acta* 1971, **31**:485–486.
37. Coombes RC, Powles TJ, Neville AM: **Evaluation of biochemical markers in breast cancer.** *Proc R Soc Med* 1977, **70**:843–845.
38. Maes M, Delange J, Ranjan R, Meltzer HY, Desnyder R, Cooremans W, Scharpe S: **Acute phase proteins in schizophrenia, mania and major depression: modulation by psychotropic drugs.** *Psychiatry Res* 1997, **66**:1–11.
39. Immenschuh S, Song DX, Satoh H, Muller-Eberhard U: **The type II hemopexin interleukin-6 response element predominates the transcriptional regulation of the hemopexin acute phase responsiveness.** *Biochem Biophys Res Commun* 1995, **207**:202–208.
40. Liang SC, Nickerson-Nutter C, Pittman DD, Carrier Y, Goodwin DG, Shields KM, Lambert AJ, Schelling SH, Medley QG, Ma HL, Collins M, Dunussi-Joannopoulos K, Fouser LA: **IL-22 induces an acute-phase response.** *J Immunol* 2010, **185**:5531–5538.

doi:10.1186/1556-276X-7-555
Cite this article as: Higashisaka *et al.*: Hemopexin as biomarkers for analyzing the biological responses associated with exposure to silica nanoparticles. *Nanoscale Research Letters* 2012 **7**:555.

Submit your manuscript to a SpringerOpen journal and benefit from:

- ► Convenient online submission
- ► Rigorous peer review
- ► Immediate publication on acceptance
- ► Open access: articles freely available online
- ► High visibility within the field
- ► Retaining the copyright to your article

Submit your next manuscript at ► springeropen.com

Biochemical and Biophysical Research Communications 427 (2012) 748–752

Contents lists available at SciVerse ScienceDirect

Biochemical and Biophysical Research Communications

journal homepage: www.elsevier.com/locate/ybbrc

Surface modification of amorphous nanosilica particles suppresses nanosilica-induced cytotoxicity, ROS generation, and DNA damage in various mammalian cells

Tokuyuki Yoshida [a], Yasuo Yoshioka [a,*], Keigo Matsuyama [a], Yasutaro Nakazato [a], Saeko Tochigi [a], Toshiro Hirai [a], Sayuri Kondoh [a], Kazuya Nagano [b], Yasuhiro Abe [c], Haruhiko Kamada [b,d], Shin-ichi Tsunoda [b,d], Hiromi Nabeshi [e], Tomoaki Yoshikawa [a], Yasuo Tsutsumi [a,b,d,*]

[a] Laboratory of Toxicology and Safety Science, Graduate School of Pharmaceutical Sciences, Osaka University, 1-6 Yamadaoka, Suita, Osaka 565-0871, Japan
[b] Laboratory of Biopharmaceutical Research, National Institute of Biomedical Innovation, 7-6-8 Saitoasagi, Ibaraki, Osaka 567-0085, Japan
[c] Cancer Biology Research Center, Sanford Research/USD, 2301 E. 60th Street N, Sioux Falls, SD 57104, USA
[d] The Center for Advanced Medical Engineering and Informatics, Osaka University, 1-6 Yamadaoka, Suita, Osaka 565-0871, Japan
[e] Division of Foods, National Institute of Health Sciences, 1-18-1, Kamiyoga, Setagaya-ku, Tokyo 158-8501, Japan

ARTICLE INFO

Article history:
Received 26 September 2012
Available online 5 October 2012

Keywords:
Amorphous nanosilica particle
DNA damage
Nanomaterial
Reactive oxygen species
Safety
Surface modification

ABSTRACT

Recently, nanomaterials have been utilized in various fields. In particular, amorphous nanosilica particles are increasingly being used in a range of applications, including cosmetics, food technology, and medical diagnostics. However, there is concern that the unique characteristics of nanomaterials might induce undesirable effects. The roles played by the physical characteristics of nanomaterials in cellular responses have not yet been elucidated precisely. Here, by using nanosilica particles (nSPs) with a diameter of 70 nm whose surface was either unmodified (nSP70) or modified with amine (nSP70-N) or carboxyl groups (nSP70-C), we examined the relationship between the surface properties of nSPs and cellular responses such as cytotoxicity, reactive oxygen species (ROS) generation, and DNA damage. To compare the cytotoxicity of nSP70, nSP70-N, or nSP70-C, we examined *in vitro* cell viability after nSP treatment. Although the susceptibility of each cell line to the nSPs was different, nSP70-C and nSP70-N showed lower cytotoxicity than nSP70 in all cell lines. Furthermore, the generation of ROS and induction of DNA damage in nSP70-C- and nSP70-N-treated cells were lower than those in nSP70-treated cells. These results suggest that the surface properties of nSP70 play an important role in determining its safety, and surface modification of nSP70 with amine or carboxyl groups may be useful for the development of safer nSPs. We hope that our results will contribute to the development of safer nanomaterials.

© 2012 Elsevier Inc. All rights reserved.

1. Introduction

The innovative development of nanotechnology has resulted in the creation of many nanomaterials (NMs), which are defined as materials with a diameter ⩽100 nm. For example, amorphous nanosilica particles (nSPs) are NMs that have received wide attention in a variety of industries, such as the medical, cosmetic, and food industries [1,2]. Because nSPs are relatively inexpensive and their surface is easily modified, their use is expected to become more widespread. Since, human exposure to NMs, including nSPs, will increase, the development of more effective and safer forms of NMs is urgently needed. Recent studies have reported that NMs may have unforeseen biologic effects that conventional-sized materials do not. For instance, Poland et al., have suggested that carbon nanotubes induce mesothelioma-like lesions in mice in a manner similar to crocidolite asbestos [3]. Other groups have shown that titanium dioxide nanoparticles enter brain tissue and induce the production of reactive oxygen species (ROS) and inflammation [4]. Furthermore, nSPs have been reported to induce oxidative stress, genotoxicity, and inflammation both *in vitro* and *in vivo* [5–7].

ROS generation induces undesirable biologic effects such as inflammation or genotoxicity [8], and recently, many reports have

Abbreviations: DCF, 2′7′-dichlorofluorescein; DCFH-DA, 2′7′-dichlorodihydorofluorescein diacetate; D-MEM, Dulbecco's modified Eagle's medium; LDH, lactate dehydrogenase; NMs, nanomaterials; nSPs, nanosilica particles; ROS, reactive oxygen species; SD, standard deviation.

* Corresponding authors. Address: Laboratory of Toxicology and Safety Science, Graduate School of Pharmaceutical Sciences, Osaka University, 1-6 Yamadaoka, Suita, Osaka 565-0871, Japan (Y. Tsutsumi). Fax: +81 6 6879 8234.

E-mail addresses: yasuo@phs.osaka-u.ac.jp (Y. Yoshioka), ytsutsumi@phs.osaka-u.ac.jp (Y. Tsutsumi).

0006-291X/$ - see front matter © 2012 Elsevier Inc. All rights reserved.
http://dx.doi.org/10.1016/j.bbrc.2012.09.132

suggested that various NM-mediated cellular responses are involved in ROS generation [9–11]. We have shown that nSPs induce inflammation or DNA damage via ROS generation *in vitro* [12,13]. Therefore, a method to avoid nSP-mediated ROS generation is needed for the development of safe nSPs.

It is well known that NM-mediated biologic effects are related to the physical characteristics of NMs, such as particle size and surface properties. Previously, we showed that nSP-mediated pregnancy complications or inflammation could be avoided by surface modification of the nSP with amino or carboxyl groups [13,14]. Another group has also reported that these surface modifications reduce nSP-induced hepatic toxicity [15]. In contrast, there are few studies that assess the relationship between the surface properties of nSPs and cellular responses such as ROS generation. In this study, we examined the relationship between the surface properties of nSPs and cellular responses such as cytotoxicity, ROS generation, and DNA damage.

2. Materials and methods

2.1. Silica particles

Amorphous nSPs (external diameter, 70 nm) with surfaces that were either unmodified or modified with amine or carboxyl groups were purchased from Micromod Partikeltechnologie GmbH, Rostock, Germany (designated nSP70, nSP70-N, and nSP70-C, respectively). The nSPs were sonicated for 5 min and vortexed for 1 min immediately prior to use.

2.2. Cell culture

HaCaT cells (human keratinocyte cell line) were kindly provided by Dr. Inui, Osaka University, Japan [16]. C8-B4 cells (murine microglial cell line), PC12 cells (rat pheochromocytoma cell line), and IEC-6 cells (rat normal small intestinal cell line) were obtained from American Type Culture Center (ATCC, Manassas, VA). TLR-1 cells (murine hepatocyte cell line) were provided by the Cell Resource Center for Biomedical Research, Institute of Development, Aging and Cancer, Tohoku University, Japan. HaCaT cells were cultured in Dulbecco's modified Eagle's medium (D-MEM; Wako, Osaka, Japan) supplemented with 10% heat-inactivated fetal bovine serum, 0.2 mM L-glutamine, and 1% Antibiotic–Antimycotic Mix stock solution. C8-B4 cells were cultured in D-MEM supplemented with 10% heat-inactivated fetal bovine serum, and 1% Antibiotic–Antimycotic Mix stock solution. PC12 cells were cultured in RPMI-1640 medium (Wako) supplemented with 10% heat-inactivated fetal bovine serum, 10% heat-inactivated horse serum, and 1% Antibiotic–Antimycotic Mix stock solution. IEC-6 cells were cultured in D-MEM supplemented with 10% heat-inactivated fetal bovine serum, 1 μg/mL insulin (Sigma–Aldrich, Saint Louis, MO), and 1% Antibiotic–Antimycotic Mix stock solution. These cell lines were grown in a humidified incubator at 37 °C (95% room air, 5% CO_2). TLR-1 cells were cultured in RITC80-7 medium supplemented with 10 μg/mL transferrin, 1 μg/mL insulin, 10 ng/mL human Epidermal Growth Factor (Sigma–Aldrich), and 1% Antibiotic–Antimycotic Mix stock solution. The cells were grown in a humidified incubator at 33 °C (95% room air, 5% CO_2).

2.3. ^{3}H-thymidine incorporation assay

The cytotoxicity of the nSP70s against C8-B4 cells, PC12 cells, IEC-6 cells, and TLR-1 cells was measured by using a ^{3}H-thymidine incorporation assay. Cells (2×10^4 cells/well seeded in 96-well plates) were cultured with various concentrations of nSP70, nSP70-C, or nSP70-N for 18 h at 37 °C; ^{3}H-thymidine (1 μCi/well) was then added into each well. After a further 6 h, cells were harvested and lysed on glass fiber filter plates using a cell harvester (PerkinElmer, Waltham, MA). The filter plates were then dried and counted by standard liquid scintillation counting techniques in a microplate counter (TopCount; PerkinElmer).

2.4. Lactate dehydrogenase release assay

The cytotoxicity of the nSP70s against HaCaT cells was evaluated by measurement of lactate dehydrogenase (LDH) release. Cells (5×10^3 cells/well seeded in a 96-well plate) were cultured with various concentrations of nSP70, nSP70-C, nSP70-N, or 0.2% Tween 20 (positive control) for 24 h at 37 °C. LDH activity of the supernatant of the culture medium was then determined using a commercial LDH cytotoxicity test (Wako) according to the manufacturer's instructions.

2.5. Detection of ROS

The generation of total intracellular ROS in HaCaT cells and TLR-1 cells was measured by monitoring the increasing fluorescence of 2′7′-dichlorofluorescein (DCF). The cell permeant 2′7′-dichlorodihydorofluorescein diacetate (DCFH-DA; Sigma–Aldrich) enters cells where intracellular esterases cleave off the diacetate group. The resulting DCFH is retained in the cytoplasm and oxidized to DCF by ROS. Cells (3×10^4 cells/well seeded in a 96-well plate) were cultured for 24 h and then treated with various concentrations of nSP70, nSP70-C, or nSP70-N for 3 h at 37 °C. Cells were then washed once with phenol red-free medium, and incubated in 100 μL of a working solution of DCFH-DA at 37 °C for 30 min. Using a fluorescence reader (ARVO MX; Perkin Elmer), the fluorescence of DCF was monitored at the excitation and emission wavelengths of 485 and 530 nm, respectively.

2.6. Comet assay

Damage of endogenous DNA in HaCaT cells after treatment with nSP70, nSP70-C, or nSP70-N was analyzed by using a Comet Assay Kit (Trevigen, Gaitherburg, MD, USA) as described previously [12,17,18]. HaCaT cells (3×10^4 cells/well seeded in a 6-well plate) were cultured for 24 h; cells were then treated with 30 μg/mL nSP70, nSP70-C, nSP70-N, or PBS (negative control) for 3 h. Cells from each group were resuspended at a density of 1×10^5 cells/mL in ice-cold calcium- and magnesium-free-PBS and combined with molten Low Melting Agarose (Trevigen) at a ratio of 1:10 (v/v). The cell–agarose mixture was immediately pipetted onto a frosted microscope slide (Comet Slide; Trevigen). Each slide was then placed flat at 4 °C in the dark for 60 min, immersed in prechilled lysis solution (Trevigen), and left at 4 °C for 40 min to remove cellular proteins and leave the DNA molecules exposed. The slides were then immersed in an alkaline solution (pH > 13, 0.3 M NaOH and 1 mM EDTA) for 40 min to denature the DNA and hydrolyze the sites that were damaged. The samples were electrophoresed for 10 min and stained with SYBR green I (Trevigen) according to the manufacturer's instructions. Twenty-five cells on each slide, which were randomly selected by use of fluorescence microscopy, were then analyzed by using a Comet Analyzer (Youworks, Tokyo, Japan). All steps were conducted under dim yellow light to prevent additional DNA damage.

2.7. Statistical analysis

All results are presented as means ± standard deviation (SD). Differences were compared by using Tukey's method after analysis of variance (ANOVA).

3. Results

To assess the relationship between the surface properties of nSPs and cellular responses, we used nSPs with diameters of 70 nm whose surface was either left unmodified (nSP70) or was chemically modified with amine (nSP70-N) or carboxyl groups (nSP70-C). In a previous study, the mean secondary particle diameter of each type of nSP was shown to be 64.2, 72.7, and 76.2 nm (nSP70, nSP70-N, and nSP70-C, respectively) [19]. The surface charge (zeta potential) of each type of silica particle was -42.1 mV, -29.8 mV, and -72.0 mV (nSP70, nSP70-N, and nSP70-C, respectively) [19].

To compare the cytotoxicity of nSP70, nSP70-N, and nSP70-C, we used a $_3$H-thymidine incorporation assay to examine cell proliferation after treatment with the nSP70s in TLR-1 cells (murine hepatocyte cell line), C8-B4 cells (murine microglial cell line), PC12 cells (rat pheochromocytoma cell line), and IEC-6 cells (rat normal small intestinal cell line). The doubling time of HaCaT cells (human keratinocyte cell line) was long, so evaluation of cytotoxicity by means of $_3$H-thymidine incorporation was unsuitable. Therefore, we examined cytotoxicity in HaCaT cells by using an LDH release assay. Although the susceptibility of each cell to the nSPs was different, nSP70 showed higher cytotoxicity than nSP70-C and nSP70-N in all cell lines (Fig. 1A–E).

Previously, we showed that nSP70 enters keratinocyte cells, and translocates to tissues throughout the whole body, such as liver, after dermal exposure in mice [18]. Therefore, we focused on HaCaT cells (keratinocyte cells) and TLR-1 cells (hepatocyte cells) to evaluate the effect of surface modification of nSP70 on ROS generation and DNA damage. Total intracellular ROS generation was measured in nSP70-, nSP70-N-, or nSP70-C-treated HaCaT cells or TLR-1 cells by assessing 2′7′-dichlorofluorescein fluorescence. In both cell lines, nSP70 induced intracellular ROS generation in a dose-dependent fashion (Fig. 2A and B). In contrast, generation of ROS by nSP70-N or nSP70-C treatment was significantly lower in both cells compared with nSP70 treatment at the same concentration (Fig. 2A and B).

In a previous study, we showed that nSP70-induced ROS generation resulted in DNA damage in HaCaT cells [12]. We therefore analyzed DNA damage in nSP70-, nSP70-N-, or nSP70-C-treated HaCaT cells by using a comet assay. The DNA damage was evaluated by tail length (Fig. 3A) and tail moment (Fig. 3B), which were defined as the product of the comet length and the amount of DNA in the tail, and the ratio of the tail length to head diameter (Fig. 3C). In cells treated with nSP70, DNA damage was induced significantly compared to negative control cells (PBS treated cells) (Fig. 3A–C). In contrast, in the nSP70-N- or nSP70-C-treated cells, DNA damage was significantly lower than that in nSP70-treated cells, and the levels of DNA damage were equal to that of negative control cells (Fig. 3A–C).

Taken together, these results indicate that the undesirable cellular effects of nSP70, such as cytotoxicity, ROS generation, and DNA damage, are reduced by surface modification of the nSP.

4. Discussion

Recently, the biodistribution of NMs through different exposure pathways has been revealed. For example, some reports have shown that NMs enter through neuronal pathways such as the olfactory bulb–brain translocation pathway [20–22]. In a previous study, we showed that after intravenous administration nSP70 tends to accumulate in the liver [18]. Thus, it is important to gather safety information on NMs using *in vitro* tests and cell lines from a range of tissues.

In the current study, we used five cell lines to show that surface modification of nSPs reduces cytotoxicity, ROS generation, and

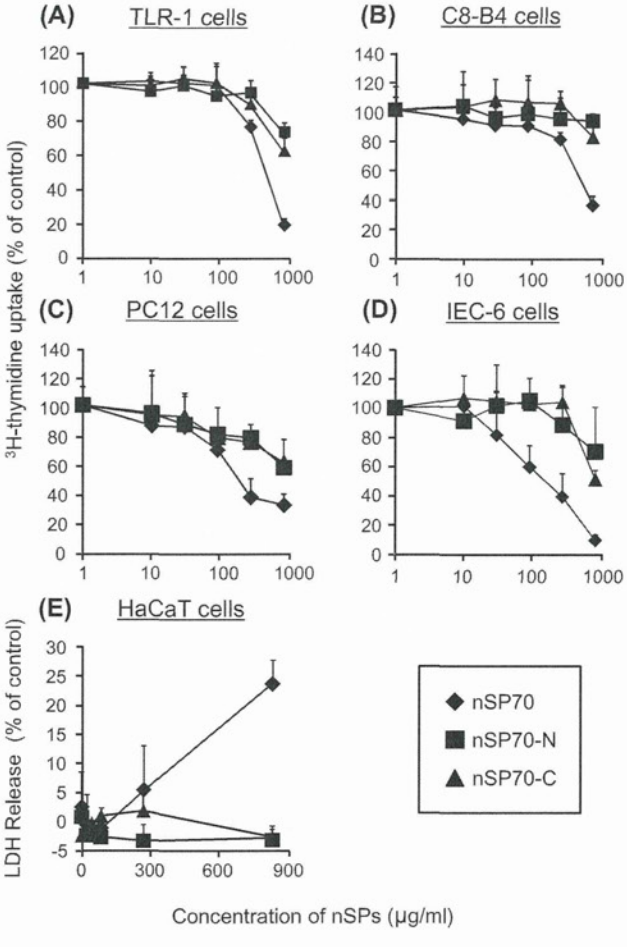

Fig. 1. Effect of surface modification of nSP70 on cytotoxicity. The cytotoxicity of (A) TLR-1 cells, (B) C8-B4 cells, (C) PC12 cells, (D) IEC-6 cells, and (E) HaCaT cells after incubation with nSP70, nSP70-N, or nSP70-C at various concentrations for 24 h was evaluated by use of a ^{3}H-thymidine incorporation assay an LDH release assay. The percentage increase in cell proliferation was calculated relative to the negative (medium) control. Data are presented as means ± SD.

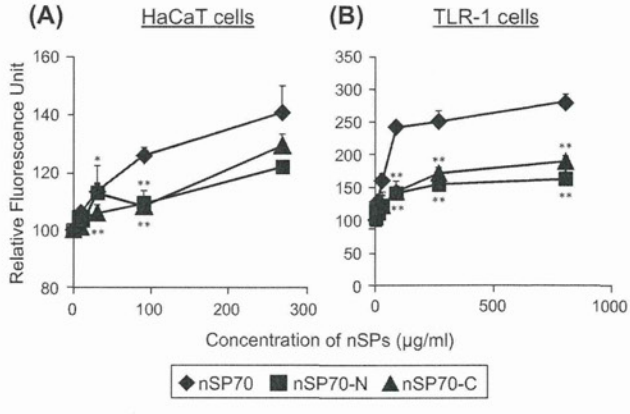

Fig. 2. Effect of surface modification of nSP70 on total ROS generation. Total ROS generation in (A) HaCaT cells and (B) TLR-1 cells incubated with nSP70, nSP70-N, or nSP70-C at various concentrations for 3 h was assessed by using a 2′7′-dichlorodihydorofluorescein assay. Total ROS induced by treatment with nSP70s is expressed as relative fluorescence units. Data are presented as means ± SD. $^{**}P < 0.01$, $^{*}P < 0.05$ vs value for same dose of nSP70.

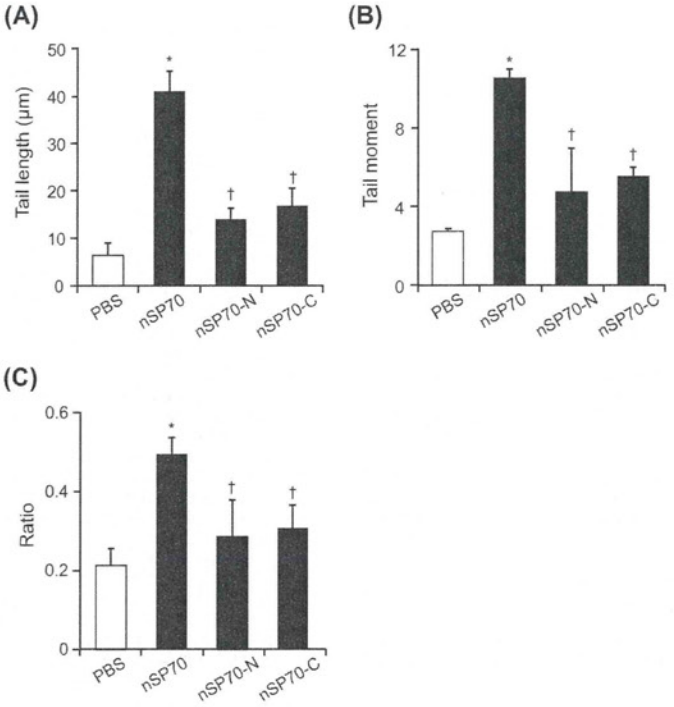

Fig. 3. Effect of surface modification of nSPs on DNA damage in HaCaT cells. HaCaT cells were incubated with nSP70, nSP70-N, or nSP70-C at 90 μg/mL for 3 h. The DNA damage was measured by (A) the tail length, (B) the tail moment, and (C) the ratio of tail length to head diameter by use of a comet assay. Data are presented as means ± SD. *$P < 0.01$ vs value for negative (PBS) control, †$P < 0.05$ vs same dose of nSP70.

DNA damage. It has been suggested that one of the factors in NM-mediated cellular responses is the cellular uptake or distribution of NMs based on their interactions with biologic proteins [23–25]. Previously, we found that although unmodified nSP70 and nSP70-C were taken up equally into cells, only nSP70 induced inflammatory responses *in vitro* [13]. Therefore, we speculated that each nSP was taken up into various cells equally in this study. On the other hand, we showed that differences in the cytotoxicity of nSP70, nSP70-N, or nSP70-C in mouse macrophage cells might be attributed to the different cellular distributions of each nSP [19]. We next plan to precisely examine the relationship among the cellular uptake/distribution of nSP70s, ROS generation and DNA damage.

ROS are primary mediators of DNA damage [26,27]. Previously, we showed that activation of NADPH oxidase, which is an important enzymatic source of ROS [28], via phagocytosis of nSP70 is a factor in DNA damage [12,29]. Therefore, we speculated that the surface modification of nSPs alter the level of activation of NADPH oxidase, and this result in the reduction of nSP70-C and -N induced-ROS generation and DNA damage. We plan to examine the relationship between NADPH oxidase activation and surface modification of nSPs; this information will help in the creation of safer forms of nSPs.

In summary, our results indicate that modification of the surface of nSPs with amine or carboxyl groups may be effective for the creation of safer nSPs. We hope that our studies will contribute to improving the safety of NMs.

Acknowledgments

This study was supported, in part, by Grants-in-Aid for Scientific Research from the Ministry of Education, Culture, Sports, Science and Technology of Japan (MEXT) and from the Japan Society for the Promotion of Science (JSPS); and by the Knowledge Cluster Initiative (MEXT); by Health Labour Sciences Research Grants from the Ministry of Health, Labour and Welfare of Japan (MHLW); by a Global Environment Research Fund from the Ministry of the Environment; by Food Safety Commission (Cabinet Office); by The Cosmetology Research Foundation; by The Smoking Research Foundation; and by The Takeda Science Foundation.

References

[1] T.K. Barik, B. Sahu, V. Swain, Nanosilica-from medicine to pest control, Parasitol. Res. 103 (2008) 253–258.
[2] D. Knopp, D. Tang, R. Niessner, Review: bioanalytical applications of biomolecule-functionalized nanometer-sized doped silica particles, Anal. Chim. Acta 647 (2009) 14–30.
[3] C.A. Poland, R. Duffin, I. Kinloch, A. Maynard, W.A. Wallace, A. Seaton, V. Stone, S. Brown, W. Macnee, K. Donaldson, Carbon nanotubes introduced into the abdominal cavity of mice show asbestos-like pathogenicity in a pilot study, Nat. Nanotechnol. 3 (2008) 423–428.
[4] J. Wang, Y. Liu, F. Jiao, F. Lao, W. Li, Y. Gu, Y. Li, C. Ge, G. Zhou, B. Li, Y. Zhao, Z. Chai, C. Chen, Time-dependent translocation and potential impairment on central nervous system by intranasally instilled TiO(2) nanoparticles, Toxicology 254 (2008) 82–90.
[5] Z. Chen, H. Meng, G. Xing, H. Yuan, F. Zhao, R. Liu, X. Chang, X. Gao, T. Wang, G. Jia, C. Ye, Z. Chai, Y. Zhao, Age-related differences in pulmonary and cardiovascular responses to SiO2 nanoparticle inhalation: nanotoxicity has susceptible population, Environ. Sci. Technol. 42 (2008) 8985–8992.
[6] X. Liu, J. Sun, Endothelial cells dysfunction induced by silica nanoparticles through oxidative stress via JNK/P53 and NF-kappaB pathways, Biomaterials 31 (2010) 8198–8209.
[7] A.T. Bauer, E.A. Strozyk, C. Gorzelanny, C. Westerhausen, A. Desch, M.F. Schneider, S.W. Schneider, Cytotoxicity of silica nanoparticles through exocytosis of von Willebrand factor and necrotic cell death in primary human endothelial cells, Biomaterials 32 (2011) 8385–8393.
[8] A.M. Knaapen, P.J. Borm, C. Albrecht, R.P. Schins, Inhaled particles and lung cancer. Part A: mechanisms, Int. J. Cancer 109 (2004) 799–809.
[9] P.V. Asha Rani, G. Low Kah Mun, M.P. Hande, S. Valiyaveettil, Cytotoxicity and genotoxicity of silver nanoparticles in human cells, ACS Nano 3 (2009) 279–290.
[10] B. Fubini, M. Ghiazza, I. Fenoglio, Physico-chemical features of engineered nanoparticles relevant to their toxicity, Nanotoxicology 4 (2010) 347–363.
[11] A. Pietroiusti, M. Massimiani, I. Fenoglio, M. Colonna, F. Valentini, G. Palleschi, A. Camaioni, A. Magrini, G. Siracusa, A. Bergamaschi, A. Sgambato, L.

Campagnolo, Low doses of pristine and oxidized single-wall carbon nanotubes affect mammalian embryonic development, ACS Nano 5 (2011) 4624–4633.
[12] H. Nabeshi, T. Yoshikawa, K. Matsuyama, Y. Nakazato, S. Tochigi, S. Kondoh, T. Hirai, T. Akase, K. Nagano, Y. Abe, Y. Yoshioka, H. Kamada, N. Itoh, S. Tsunoda, Y. Tsutsumi, Amorphous nanosilica induce endocytosis-dependent ROS generation and DNA damage in human keratinocytes, Part. Fibre Toxicol. 8 (2011) 1.
[13] T. Morishige, Y. Yoshioka, H. Inakura, A. Tanabe, S. Narimatsu, X. Yao, Y. Monobe, T. Imazawa, S. Tsunoda, Y. Tsutsumi, Y. Mukai, N. Okada, S. Nakagawa, Suppression of nanosilica particle-induced inflammation by surface modification of the particles, Arch. Toxicol. 86 (2012) 1297–1307.
[14] K. Yamashita, Y. Yoshioka, K. Higashisaka, K. Mimura, Y. Morishita, M. Nozaki, T. Yoshida, T. Ogura, H. Nabeshi, K. Nagano, Y. Abe, H. Kamada, Y. Monobe, T. Imazawa, H. Aoshima, K. Shishido, Y. Kawai, T. Mayumi, S. Tsunoda, N. Itoh, T. Yoshikawa, I. Yanagihara, S. Saito, Y. Tsutsumi, Silica and titanium dioxide nanoparticles cause pregnancy complications in mice, Nat. Nanotechnol. 6 (2011) 321–328.
[15] K. Isoda, T. Hasezaki, M. Kondoh, Y. Tsutsumi, K. Yagi, Effect of surface charge on nano-sized silica particles-induced liver injury, Pharmazie 66 (2011) 278–281.
[16] S. Inui, Y.F. Lee, A.R. Haake, L.A. Goldsmith, C. Chang, Induction of TR4 orphan receptor by retinoic acid in human HaCaT keratinocytes, J. Invest. Dermatol. 112 (1999) 426–431.
[17] K. Yamashita, Y. Yoshioka, K. Higashisaka, Y. Morishita, T. Yoshida, M. Fujimura, H. Kayamuro, H. Nabeshi, T. Yamashita, K. Nagano, Y. Abe, H. Kamada, Y. Kawai, T. Mayumi, T. Yoshikawa, N. Itoh, S. Tsunoda, Y. Tsutsumi, Carbon nanotubes elicit DNA damage and inflammatory response relative to their size and shape, Inflammation 33 (2010) 276–280.
[18] H. Nabeshi, T. Yoshikawa, K. Matsuyama, Y. Nakazato, K. Matsuo, A. Arimori, M. Isobe, S. Tochigi, S. Kondoh, T. Hirai, T. Akase, T. Yamashita, K. Yamashita, T. Yoshida, K. Nagano, Y. Abe, Y. Yoshioka, H. Kamada, T. Imazawa, N. Itoh, S. Nakagawa, T. Mayumi, S. Tsunoda, Y. Tsutsumi, Systemic distribution, nuclear entry and cytotoxicity of amorphous nanosilica following topical application, Biomaterials 32 (2011) 2713–2724.
[19] H. Nabeshi, T. Yoshikawa, A. Arimori, T. Yoshida, S. Tochigi, T. Hirai, T. Akase, K. Nagano, Y. Abe, H. Kamada, S. Tsunoda, N. Itoh, Y. Yoshioka, Y. Tsutsumi, Effect of surface properties of silica nanoparticles on their cytotoxicity and cellular distribution in murine macrophages, Nanoscale Res. Lett. 6 (2011) 93.
[20] Q. Liu, X. Shao, J. Chen, Y. Shen, C. Feng, X. Gao, Y. Zhao, J. Li, Q. Zhang, X. Jiang, In vivo toxicity and immunogenicity of wheat germ agglutinin conjugated poly(ethylene glycol)-poly(lactic acid) nanoparticles for intranasal delivery to the brain, Toxicol. Appl. Pharmacol. 251 (2011) 79–84.
[21] H. Xia, X. Gao, G. Gu, Z. Liu, N. Zeng, Q. Hu, Q. Song, L. Yao, Z. Pang, X. Jiang, J. Chen, H. Chen, Low molecular weight protamine-functionalized nanoparticles for drug delivery to the brain after intranasal administration, Biomaterials 32 (2011) 9888–9898.
[22] Y.Y. Kao, T.J. Cheng, D.M. Yang, C.T. Wang, Y.M. Chiung, P.S. Liu, Demonstration of an olfactory bulb-brain translocation pathway for ZnO nanoparticles in rodent cells in vitro and in vivo, J. Mol. Neurosci. 48 (2012) 464–471.
[23] A.E. Nel, L. Madler, D. Velegol, T. Xia, E.M. Hoek, P. Somasundaran, F. Klaessig, V. Castranova, M. Thompson, Understanding biophysicochemical interactions at the nano-bio interface, Nat. Mater. 8 (2009) 543–557.
[24] C. Ge, J. Du, L. Zhao, L. Wang, Y. Liu, D. Li, Y. Yang, R. Zhou, Y. Zhao, Z. Chai, C. Chen, Binding of blood proteins to carbon nanotubes reduces cytotoxicity, Proc. Nat. Acad. Sci. USA 108 (2011) 16968–16973.
[25] M.P. Monopoli, F.B. Bombelli, K.A. Dawson, Nanobiotechnology: nanoparticle coronas take shape, Nat. Nanotechnol. 6 (2011) 11–12.
[26] D. Harman, The aging process, Proc. Nat. Acad. Sci. USA 78 (1981) 7124–7128.
[27] B.N. Ames, Dietary carcinogens and anticarcinogens. Oxygen radicals and degenerative diseases, Science 221 (1983) 1256–1264.
[28] F. Morel, J. Doussiere, P.V. Vignais, The superoxide-generating oxidase of phagocytic cells. Physiological, molecular and pathological aspects, Eur. J. Biochem. 201 (1991) 523–546.
[29] T. Morishige, Y. Yoshioka, H. Inakura, A. Tanabe, X. Yao, S. Narimatsu, Y. Monobe, T. Imazawa, S. Tsunoda, Y. Tsutsumi, Y. Mukai, N. Okada, S. Nakagawa, The effect of surface modification of amorphous silica particles on NLRP3 inflammasome mediated IL-1beta production, ROS production and endosomal rupture, Biomaterials 31 (2010) 6833–6842.

Laboratory of Toxicology and Safety Science[1], Graduate School of Pharmaceutical Sciences; Laboratory of Biopharmaceutical Research[2], National Institute of Biomedical Innovation, Osaka, Japan; Cancer Biology Research Center[3], Sanford Research/USD, Sioux Falls, SD, USA; The Center for Advanced Medical Engineering and Informatics[4], Osaka University; Vitamin C60 BioResearch Corporation[5]; Division of Foods[6], National Institute of Health Sciences, Tokyo, Japan

Biochemical and hematologic effects of polyvinylpyrrolidone-wrapped fullerene C_{60} after oral administration

K. YAMASHITA[1], Y. YOSHIOKA[1], H. PAN[1], M. TAIRA[1], T. OGURA[1], T. NAGANO[1], M. AOYAMA[1], K. NAGANO[2], Y. ABE[3], H. KAMADA[2,4], S.-I. TSUNODA[2,4], H. AOSHIMA[5], H. NABESHI[6], T. YOSHIKAWA[1], Y. TSUTSUMI[1,2,4]

Received July 12, 2012, accepted August 10, 2012

Yasuo Yoshioka, PhD and Yasuo Tsutsumi, Ph.D, Laboratory of Toxicology and Safety Science, Graduate School of Pharmaceutical Sciences, Osaka University, 1-6 Yamadaoka, Suita, Osaka, 565-0871, Japan
yasuo@phs.osaka-u.ac.jp; ytsutsumi@phs.osaka-u.ac.jp

Pharmazie 68: 54–57 (2013) *doi: 10.1691/ph.2013.2708*

The fullerene C_{60} is used in consumer products such as cosmetics owing to its antioxidative effects and is being developed for nanomedical applications. However, knowledge regarding the safety of fullerene C_{60}, especially after oral administration, is sparse. Here, we examined the safety of fullerene C_{60} in mice after 7 d of exposure to orally administered polyvinylpyrrolidone (PVP)-wrapped fullerene C_{60} (PVP-fullerene C_{60}). Mice treated with PVP-fullerene C_{60} showed few changes in the plasma levels of various markers of kidney and liver injury and experienced no significant hematologic effects. Furthermore, the histology of the colon of PVP-fullerene C_{60}-treated mice was indistinguishable from that of control mice. These results suggest that PVP-fullerene C_{60} lacks toxicity after high-dose oral administration and indicate that PVP-fullerene C_{60} can be considered safe for oral medication. These data provide basic information that likely will facilitate the production of safe and effective forms of fullerene C_{60}.

1. Introduction

Advances in nanotechnology have led to the recent development of many nanomaterials, including nanoscale silica particles, titanium dioxide nanoparticles, and carbon nanomaterials (Augustin and Sanguansri 2009; Bowman et al. 2010; Konstantatos and Sargent 2010; Petros and DeSimone 2010). Nanomaterials typically are defined as materials that are 1 to 100 nm in length or diameter. Compared with micro-sized particles, nanomaterials have a high surface area, with increased structural integrity and unique mechanical, chemical, electrical, and magnetic properties. These properties have led to the use of nanomaterials in electronics, foods, and cosmetics and as drug delivery vehicles (Augustin and Sanguansri 2009; Bowman et al. 2010; Konstantatos and Sargent 2010; Petros and DeSimone 2010).

The fullerene C_{60} is one of the most promising nanomaterials because of its unique chemical and physical properties (Chen et al. 2012). Fullerene C_{60} is a remarkably stable compound consisting of 60 carbon atoms, with a diameter of approximately 0.7 nm. Thirty carbon double bonds are present in the structure, to which free radicals easily bond, leading to fullerene C_{60}'s characterization as a "radical sponge" (Krusic et al. 1991). Because of this strong antioxidative feature, fullerene C_{60} is used in cosmetics to reduce oxidative stress in the skin (Benn et al. 2011; Kato et al. 2010). In addition, various water-soluble fullerene C_{60} derivatives have been synthesized for use in a wide range of biologic applications (Aoshima et al. 2009; Kokubo et al. 2008; Lin and Lu 2012; Yin et al. 2009). For example, water-soluble fullerene C_{60} has stronger antimelanogenic potential than do naturally occurring whitening agents (Kato et al. 2009; Xiao et al. 2007). Furthermore, water-soluble fullerene C_{60} derivatives show promise for the treatment of various inflammatory diseases including rheumatoid arthritis (Hu et al. 2007; Yudoh et al. 2009a,b). Because of these potential biologic applications, several studies have assessed the safety of fullerene C_{60} and its water-soluble derivatives (Aoshima et al. 2010; Kato et al; 2009).

One water-soluble derivative, polyvinylpyrrolidone (PVP)-wrapped fullerene C_{60} (PVP-fullerene C_{60}), is used as a very stable, strongly antioxidative ingredient of cosmetics (Aoshima et al. 2010; Xiao et al. 2007). When applied to the skin, PVP-fullerene C_{60} exhibits protective activity against the apoptosis of keratinocytes that is caused by reactive oxygen species (Xiao et al. 2007). Furthermore, *in vitro* chromosomal aberration assays were conducted using mammalian cells and negative results were reported for PVP-fullerene C_{60} (Aoshima et al. 2010). However, only a few studies have addressed the safety of orally administered PVP-fullerene C_{60} *in vivo*. Therefore assessment of the safety of PVP-fullerene C_{60} after oral administration is a key area in the development of nanomedicines using PVP-fullerene C_{60}.

Here, we examined the safety of PVP-fullerene C_{60} after oral administration to mice. Our data show that oral administration of PVP-fullerene C_{60} induced negligible changes in various biochemical and hematologic parameters. These data provide useful basic safety information that likely will facilitate the development of safe and effective forms of fullerene C_{60}.

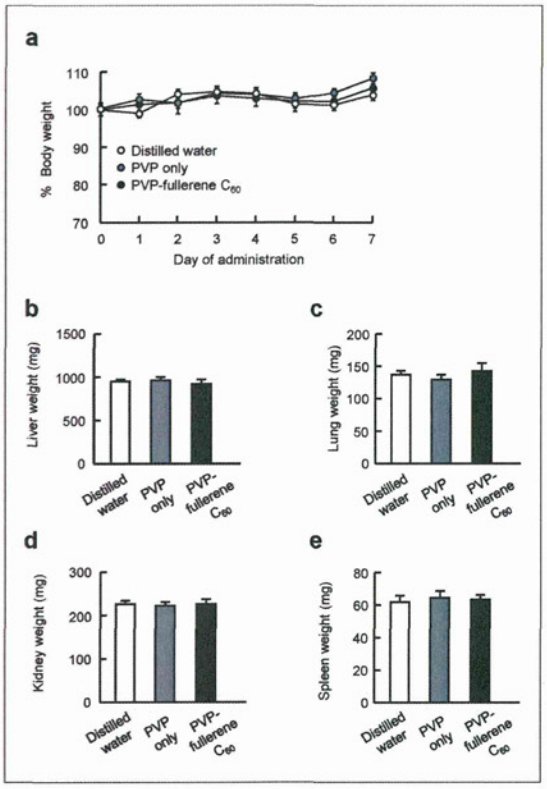

Fig. 1: Effect of oral administration of PVP-fullerene C_{60} on body weight and wet organ weights of mice. PVP-fullerene C_{60} solution in distilled water (50 mg/500 μL/mouse) was administrated orally. Control mice received distilled water or PVP only; all mice were treated by oral gavage daily for 7 d. (a) Body weight during oral administration of PVP-fullerene C_{60}, PVP only, or distilled water. Wet weight of (b) liver, (c) lung, (d) kidney, and (e) spleen after 7 d of treatment. Data are given as mean ± SEM (n = 8)

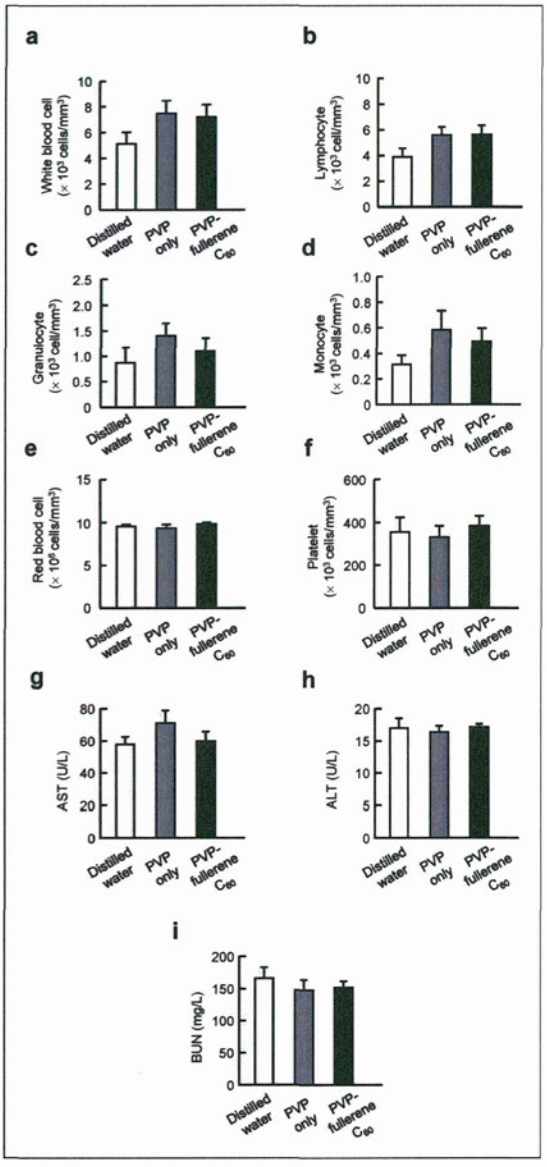

Fig. 2: Effect of oral administration of PVP-fullerene C_{60} on hematologic and biochemical parameters of mice. (a–f) Hematologic parameters were measured after oral administration of PVP-fullerene C_{60} for 7 d. (g–i) Biochemical parameters in the plasma were measured after oral administration of PVP-fullerene C_{60} for 7 d. Data are given as mean ± SEM (n = 6 or 7)

2. Investigations, results and discussion

We first used dynamic light scattering to measure the hydrodynamic diameters of PVP-fullerene C_{60}. The particle size of PVP-fullerene C_{60} in the distilled water was 127 nm, and its zeta potential was –2.2 mV.

To examine the safety of PVP-fullerene C_{60} after oral administration to mice, each mouse received 0.5 ml of distilled water, PVP only, or PVP-fullerene C_{60} solution by oral gavage once daily for 7 d. Daily behavior including eating, drinking, and activity did not differ between groups; no mice died; and there were no overt differences in body weight gain between groups (Fig. 1a). In addition, wet organ weight after 7 d of oral treatment did not differ significantly between groups (Fig. 1b–e). Hematologic parameters including numbers of red blood cells, platelets, white blood cells, lymphocytes, granulocytes, and monocytes in mice did not show significant differences between groups (Fig. 2a–f). Similarly, plasma biochemical parameters including aspartate aminotransferase (AST) and alanine aminotransferase (ALT) as indicators of hepatic injury and blood urea nitrogen (BUN) as a marker of renal damage did not differ significantly between groups (Fig. 2g–i).

Disease symptom scores and colon length are well-known indicators of colonic inflammation, which is the most common adverse effect after oral administration of test compounds. We scored fecal occult blood as a disease symptom in mice. Similar to those for the distilled water group (1.6 ± 0.1) or PVP only group (1.5 ± 0.1), the score for the PVP-fullerene C_{60}-treated group (1.5 ± 0.1) did not indicate any occult or gross rectal bleeding (Fig. 3a). Furthermore neither colon length (Fig. 3b) nor histology (Fig. 3c–e) differed between groups. Taking together all of our results, we consider that oral administration of 50 mg PVP-fullerene C_{60} daily for 7 d has negligible effects on the health of the colon in mice (Fig. 3).

Various *in vitro* and *in vivo* safety assessments of fullerene C_{60} and its derivatives have been reported previously (Metanawin et al. 2011; Nielsen et al. 2008; Zhang et al. 2009). Most studies have shown that fullerene C_{60} and its derivatives are not genotoxic under *in vitro* conditions (Aoshima et al. 2010; Ema

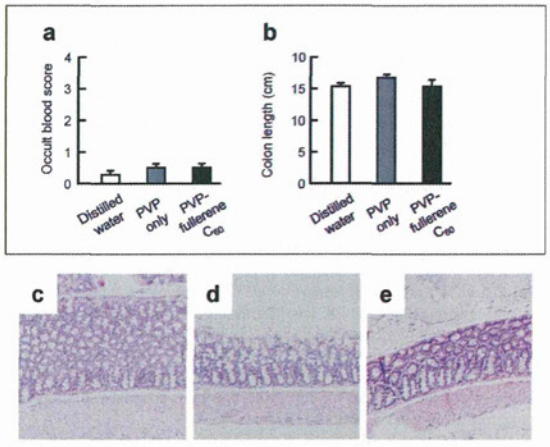

Fig. 3: Effect of oral administration of PVP-fullerene C_{60} on the histology of the colon in mice. (a) Occult blood scores were determined after 7 d of treatment by assessing the consistency, overt blood, and occult blood of feces. (b) Effect of PVP-fullerene C_{60} on colon length. All data are expressed as mean ± SEM (n = 8). Histopathology of the distal colon in C57/BL6 mice after oral administration of distilled water (c), PVP only (d) or PVP-fullerene C_{60} (e) for 7 d. Representative sections were stained with hematoxylin and eosin and examined by using light microscopy

et al. 2012; Shinohara et al. 2009). In addition, water-soluble fullerene C_{60} derivatives can safely be used for dermal and intraperitoneal injection (Aoshima et al. 2010; Gharbi et al. 2005). However, insufficient information is available regarding the safety of water-soluble fullerene C_{60} derivatives after oral administration. In this study, we evaluated the safety and toxicity of oral PVP-fullerene C_{60} by monitoring the body weight, hematologic and biochemical parameters, and colonic health of treated mice. Our results indicate that oral PVP-fullerene C_{60} has no adverse effects on the evaluated parameters in mice.

Guidelines from the Organization for Economic Co-operation and Development (OECD) recommend 28- and 90-d repeated-dose oral toxicity studies in rodents for the safety assessment of chemicals used as nanomaterials. As a first step in the safety assessment of PVP-fullerene C_{60}, we here performed a 7-d oral toxicity study. Now we are trying to perform safety evaluations after long-term exposure.

In conclusion, we showed that oral administration of PVP-fullerene C_{60} induced negligible change in various hematologic, biochemical, and histologic parameters in mice. Although additional studies are needed to further examine the safety of PVP-fullerene C_{60}, we consider that our data provide the basic information that likely will facilitate the development of safe and effective forms of fullerene C_{60}.

3. Experimental

3.1. Particles

PVP-fullerene C_{60} was provided by Vitamin C60 BioResearch (Tokyo, Japan) and is composed of purified fullerene C_{60} and PVP of 60 to 80 kDa. The C_{60} content in PVP-fullerene C_{60} was determined by HPLC analysis on a 5PBB column (Nacalai Tesque, Kyoto, Japan) and found to be approximately 3000 ppm. PVP-fullerene C_{60} was used after 5 min of sonication (280 W output; Ultrasonic Cleaner, AS One, Tokyo, Japan) and 1 min of vortexing. Particle size and zeta potential were measured by using a Zetasizer Nano-ZS (Malvern Instruments, Worcestershire, UK). The mean size and size distribution of particles were measured by using dynamic light scattering; zeta potential was measured by using laser doppler electrophoresis.

3.2. Mice

Female C57BL/6 mice were purchased from Nippon SLC (Kyoto, Japan) and used at 6 weeks of age. Mice were housed in a ventilated animal room maintained at 20 ± 2 °C with a 12:12-h light:dark cycle. Distilled water and sterilized mouse chow were available *ad libitum*. All procedures were performed in accordance with institutional ethical guidelines for animal experiments. During the treatment period, each mouse received 0.5 ml distilled water, PVP only, or PVP-fullerene C_{60} in distilled water (total dose, 50 mg) by oral gavage once daily for 7 d. Mice were euthanized 24 h after administration of the final dose, and liver, lung, kidney, and spleen tissues were harvested and weighed. Blood samples were collected in tubes containing 5 IU/ml heparin sodium, and plasma was harvested. Colons were resected for the determination of colon length (from cecum to anus) and histopathologic examination. Feces were collected and evaluated for occult blood.

3.3. Hematologic analysis

The numbers of white blood cells, granulocytes, lymphocytes, monocytes, red blood cells, and platelets in whole blood were measured by using an auto analyzer (VetScan HMII Hematology System, Abaxis, Union City, CA). Liver function was assessed by measuring plasma levels of AST and ALT. Nephrotoxicity was evaluated by measuring plasma levels of BUN. AST, ALT, and BUN were assayed by using a biochemical autoanalyzer (Fuji Dri-Chem 7000, Fujifilm, Tokyo, Japan).

3.4. Histopathologic examination

For histology of paraffin-fixed tissue, colons were excised and fixed overnight in 10% neutral buffered formalin, embedded in paraffin blocks, sliced, and placed on glass slides. Sections were deparaffinized, rehydrated through a graded series of ethanol, and stained with hematoxylin and eosin. Stained sections were dehydrated through a graded ethanol series and mounted using permount (OCT Compound, Sakura Finetek, Tokyo, Japan). Representative histologic images were recorded by a CCD digital camera that was affixed to a microscope. Fecal occult blood was scored by using the Coloscreen Occult Blood Card Test (Shionogi, Osaka, Japan), with the scale ranging from 0 for negative to 4 for strongly positive.

3.5. Statistical analysis

All results are presented as mean ± standard error of the mean (SEM). Statistical significance in differences was evaluated by analysis of variance (ANOVA) followed by Bonferroni correction. The P value used to define significance ($P < 0.05$).

Competing interests: The authors declare that there are no conflicts of interest.

Acknowledgements: This study was supported in part by Grants-in-Aid for Scientific Research from the Ministry of Education, Culture, Sports, Science and Technology of Japan (MEXT), and from the Japan Society for the Promotion of Science (JSPS); and by a the Knowledge Cluster Initiative (MEXT); by Health Labour Sciences Research Grants from the Ministry of Health, Labor and Welfare of Japan (MHLW); by a Global Environment Research Fund from Minister of the Environment; by Food Safety Commission (Cabinet Office); by The Cosmetology Research Foundation; by The Smoking Research Foundation; by The Takeda Science Foundation; by The Nagai Foundation Tokyo; by The Research Foundation for Pharmaceutical Sciences; and by The Japan Food Chemical research Foundation.

References

Aoshima H, Kokubo K, Shirakawa S, Ito M, Yamana S, Oshima T (2009) Antimicrobial activity of fullerenes and their hydroxylated derivatives. Biocontrol Sci 14: 69–72.

Aoshima H, Yamana S, Nakamura S, Mashino T (2010) Biological safety of water-soluble fullerenes evaluated using tests for genotoxicity, phototoxicity, and pro-oxidant activity. J Toxicol Sci 35: 401–409.

Augustin MA, Sanguansri P (2009) Nanostructured materials in the food industry. Adv Food Nutr Res 58: 183–213.

Benn TM, Westerhoff P, Herckes P (2011) Detection of fullerenes (C60 and C70) in commercial cosmetics. Environ Pollut 159: 1334–1342.

Bimbo LM, Sarparanta M, Santos HA, Airaksinen AJ, Makila E, Laaksonen T, Peltonen L, Lehto VP, Hirvonen J, Salonen J (2010) Biocompatibility of thermally hydrocarbonized porous silicon nanoparticles and their biodistribution in rats. ACS Nano 4: 3023–3032.

Bowman DM, van Calster G, Friedrichs S (2010) Nanomaterials and regulation of cosmetics. Nat Nanotechnol 5: 92.

Chen Z, Ma L, Liu Y, Chen C (2012) Applications of functionalized fullerenes in tumor theranostics. Theranostics 2: 238–250.

Ema M, Tanaka J, Kobayashi N, Naya M, Endoh S, Maru J, Hosoi M, Nagai M, Nakajima M, Hayashi M, Nakanishi J (2012) Genotoxicity evaluation of fullerene C60 nanoparticles in a comet assay using lung cells of intratracheally instilled rats. Regul Toxicol Pharmacol 62: 419–424.

Gharbi N, Pressac M, Hadchouel M, Szwarc H, Wilson SR, Moussa F (2005) [60]fullerene is a powerful antioxidant in vivo with no acute or subacute toxicity. Nano Lett 5: 2578–2585.

Hu Z, Liu S, Wei Y, Tong E, Cao F, Guan W (2007) Synthesis of glutathione C60 derivative and its protective effect on hydrogen peroxide-induced apoptosis in rat pheochromocytoma cells. Neurosci Lett 429: 81–86.

Kato S, Aoshima H, Saitoh Y, Miwa N (2009) Biological safety of Lipo-Fullerene composed of squalane and fullerene-C60 upon mutagenesis, photocytotoxicity, and permeability into the human skin tissue. Basic Clin Pharmacol Toxicol 104: 483–487.

Kato S, Taira H, Aoshima H, Saitoh Y, Miwa N (2010) Clinical evaluation of *fullerene-C60 dissolved in squalane for anti-wrinkle cosmetics. J Nanosci* Nanotechnol 10: 6769–6774.

Kokubo K, Tochika S, Kato M, Sol Y, Oshima T (2008) AlCl3-catalyzed tandem acetylation of hydroarylated [60]fullerenes. Org Lett 10: 3335–3338.

Konstantatos G, Sargent EH (2010) Nanostructured materials for photon detection. Nat Nanotechnol 5: 391–400.

Krusic PJ, Wasserman E, Keizer PN, Morton JR, Preston KF (1991) Radical reactions of c60. Science 254: 1183–1185.

Lin CM, Lu TY (2012) C60 Fullerene Derivatized Nanoparticles and their Application to Therapeutics. Recent Pat Nanotechnol 6: 105–113.

Metanawin T, Tang T, Chen R, Vernon D, Wang X (2011) Cytotoxicity and photocytotoxicity of structure-defined water-soluble C60/micelle supramolecular nanoparticles. Nanotechnology 22: 235604.

Nielsen GD, Roursgaard M, Jensen KA, Poulsen SS, Larsen ST (2008) In vivo biology and toxicology of fullerenes and their derivatives. Basic Clin Pharmacol Toxicol 103: 197–208.

Petros RA, DeSimone JM (2010) Strategies in the design of nanoparticles for therapeutic applications. Nat Rev Drug Discov 9: 615–627.

Shinohara N, Matsumoto K, Endoh S, Maru J, Nakanishi J (2009) In vitro and in vivo genotoxicity tests on fullerene C60 nanoparticles. Toxicol Lett 191: 289–296.

Xiao L, Matsubayashi K, Miwa N (2007) Inhibitory effect of the water-soluble polymer-wrapped derivative of fullerene on UVA-induced melanogenesis via downregulation of tyrosinase expression in human melanocytes and skin tissues. Arch Dermatol Res 299: 245–257.

Yamago S, Tokuyama H, Nakamura E, Kikuchi K, Kananishi S, Sueki K, Nakahara H, Enomoto S, Ambe F (1995) In vivo biological behavior of a water-miscible fullerene: 14C labeling, absorption, distribution, excretion and acute toxicity. Chem Biol 2: 385–389.

Yin JJ, Lao F, Fu PP, Wamer WG, Zhao Y, Wang PC, Qiu Y, Sun B, Xing G, Dong J, Liang XJ, Chen C (2009) The scavenging of reactive oxygen species and the potential for cell protection by functionalized fullerene materials. Biomaterials 30: 611–621.

Yudoh K, Karasawa R, Masuko K, Kato T (2009a) Water-soluble fullerene (C60) inhibits the development of arthritis in the rat model of arthritis. Int J Nanomedicine 4: 217–225.

Yudoh K, Karasawa R, Masuko K, Kato T (2009b) Water-soluble fullerene (C60) inhibits the osteoclast differentiation and bone destruction in arthritis. Int J Nanomedicine 4: 233–239.

Zhang LW, Yang J, Barron AR, Monteiro-Riviere NA (2009) Endocytic mechanisms and toxicity of a functionalized fullerene in human cells. Toxicol Lett 191: 149–157.

Laboratories of Bio-Functional Molecular Chemistry[1] and Toxicology and Safety Science[2], Graduate School of Pharmaceutical Sciences, Osaka University, Japan

Hepatotoxicity of sub-nanosized platinum particles in mice

Y. YAMAGISHI[1], A. WATARI[1], Y. HAYATA[1], X. LI[1], M. KONDOH[1], Y. TSUTSUMI[2], K. YAGI[1]

Received July 19, 2012, accepted August 30, 2012

Dr. Akihiro Watari, Laboratory of Bio-Functional Molecular Chemistry, Graduate School of Pharmaceutical Sciences, Osaka University, Suita, Osaka 565-0871, Japan
akihiro@phs.osaka-u.ac.jp

Pharmazie 68: 178–182 (2013) *doi: 10.1691/ph.2013.2141*

Nano-sized materials are widely used in consumer products, medical devices and engineered pharmaceuticals. Advances in nanotechnology have resulted in materials smaller than the nanoscale, but the biologic safety of the sub-nanosized materials has not been fully assessed. In this study, we evaluated the toxic effects of sub-nanosized platinum particles (snPt) in the mouse liver. After intravenous administration of snPt (15 mg/kg body weight) into mice, histological analysis revealed acute hepatic injury, and biochemical analysis showed increased levels of serum markers of liver injury and inflammatory cytokines. In contrast, administration of nano-sized platinum particles did not produce these abnormalities. Furthermore, snPt induced cytotoxicity when directly applied to primary hepatocytes. These data suggest that snPt have the potential to induce hepatotoxicity. These findings provide useful information on the further development of sub-nanosized materials.

1. Introduction

Nanotechnology involves manipulation of matter on the scale of the nanometer and has the potential to improve quality of life via functional products. Nanomaterials are commonly defined as objects with dimensions of 1 to 100 nm and are now widely used in electronics, catalysts, clothing, drugs, diagnostic devices, and cosmetics (Baughman et al. 2002; Patra et al. 2010; Service et al. 2007; Ariga et al. 2010). Recent progress in the field has allowed the creation of sub-nanosized materials that have different physicochemical properties, including improved conductivity, durability and strength. Although these materials may be useful for industrial and scientific purposes, the biologic safety of these materials has not been fully evaluated (Nel et al. 2006; Oberdorster et al. 2005).

Nano-sized platinum particles (nPt) are used for industrial applications and in consumer products, such as cosmetics, supplements and food additives (Gehrke et al. 2011; Horie et al. 2011). The biological influence of exposure to nPt has been previously investigated. For example, nPt has anti-oxidative activity (Watanabe et al. 2009; Onizawa et al. 2009; Kajita et al. 2007), and may be useful for the medical treatment of diseases related to oxidative stress and aging. However, some reports suggest that these substances can induce inflammation in mice or impair DNA integrity (Pelka et al. 2009; Park et al. 2010). Thus, the understanding of the biological influences of nPt has still not been definitively established, and our knowledge regarding the biological effects of sub-nanosized platinum particles (snPt) is severely lacking.

Nano-sized particles can enter and penetrate the lungs, intestines and skin. The degree of penetration depends on the size and surface features of the nano-sized particle. Furthermore, nanoparticles can enter the circulatory system and migrate to various organs, such as the brain, spleen, liver, kidney and muscles (Zhu et al. 2008; Furuyama et al. 2009; Oberdorster et al. 2004; Ai et al. 2011). The liver is a vital organ that is involved in the uptake of nutrients and the elimination of waste products and pathogens from the blood; it is also an important organ for the clearance of nanoparticles. However, some nanoparticles are hepatotoxic (Nishimori et al. 2009a, b; Ji et al. 2009; Cho et al. 2009; Folkmann et al. 2009). In the present study, we investigated the influence of sub-nanosized platinum particles (snPt) on the liver.

2. Investigations and results

To investigate the acute liver toxicity of snPt, we administered snPt (15 mg/kg body weight) into mice by intravenous injection. Histological analysis revealed acute hepatic injury, including vacuole degeneration (Fig. 1). Furthermore, administration of snPt at doses over 15 mg/kg resulted in significant elevation of serum alanine aminotransferase (ALT) and aspartate aminotransferase (AST) levels (Fig. 2A and B) and of interleukin-6 (IL-6) levels (Fig. 2C). ALT and AST levels were increased at 3 h to 24 h after intravenous administration at 20 mg/kg snPt (Fig. 3A and B). Cell viability assessment by WST assay demonstrated that direct treatment of isolated hepatocytes with snPt at concentrations of 0.1, 1, 10, 50 and 100 μg/ml resulted in a dose-dependent decrease in hepatocyte viability when compared with vehicle-treated cells (Fig. 4). These observations suggest that snPt induced inflammation and hepatocyte death.

Previous reports showed that biological influences of nanomaterials vary according to material size (Nishimori et al. 2009a, b; Jiang et al. 2008; Oberdorster et al. 2010). Therefore, we examined whether nPt, with a diameter of approximately 15 nm, leads

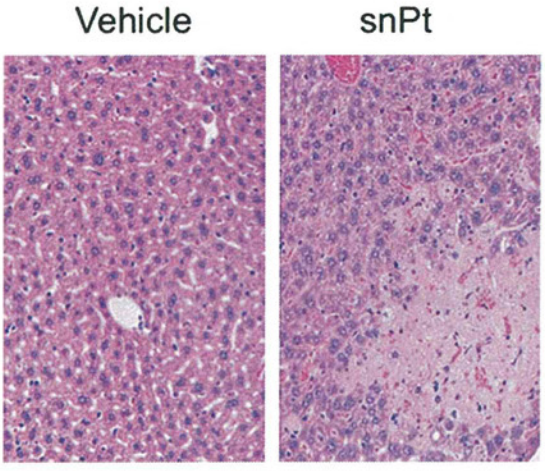

Fig. 1: Histological analysis of liver tissues in snPt-treated mice. snPt was intravenously administered to mice at 15 mg/kg. At 24 h after administration, livers were collected and fixed with 4% paraformaldehyde. Tissue sections were stained with hematoxylin and eosin and observed under a microscope. The pictures show representative data from at least four mice

to a different biologic effect than snPt. As shown in Fig. 5, snPt administration resulted in dose-dependent increases in serum ALT and AST levels, whereas nPt did not. Furthermore, IL-6 levels did not change in response to administration of nPt. These results suggest that the biological effects of platinum particles are dependent on their size.

3. Discussion

The influence of size and of physiochemical properties of nanoparticles on their biologic safety is an important issue. Animal experiments have demonstrated rapid translocation of nanoparticles from the entry site to various organs (Almeida et al. 2011). In particular, nanoparticles tend to concentrate in the liver and are cleared from the body in the feces and urine after intravenous infusion (Ai et al. 2011). While the liver plays a pivotal role in the clearance of nanoparticles, some nanomaterials can induce liver injury. Therefore, we assessed the influence of snPt on the liver and demonstrated that snPt induced liver toxicity *in vitro* and *in vivo*.

Some studies have reported that nPt exert anti-oxidant and anti-inflammatory effects (Watanabe et al. 2009; Onizawa et al. 2009; Kajita et al. 2007), while other studies reported that nPt have negative biological effects. For example, treatment of a human colon carcinoma cell line with nPt resulted in a decrease in cellular glutathione level and impairment in DNA integrity (Pelka et al. 2009). Furthermore, Park et al. (2010) found that nPt prepared from K_2PtCl_6 may induce an inflammatory response in mice. In this study, we found that snPt damaged liver tissues and induced inflammatory cytokines. Kupffer cells present in liver sinusoids may mediate this process via phagocytosis of the particles and subsequent release of inflammatory cytokines. However, when we added snPt to primary hepatocytes, the viability of the cells was significantly reduced, suggesting that snPt may also exert a direct hepatotoxic effect. Thus, the cellular influences of Pt nano- and sub-nano particles may be dependent on the target cells as well as on the size and physical and chemical properties of the particles.

snPt may damage other tissues as well. Cisplatin, a first-line chemotherapy for most cancers, is a platinating agent that can cause kidney damage (Daugaard et al. 1990; Brabec et al. 2005). Furthermore, snPt-induced increases in systemic IL-6 may cause damage to various organs. Further analysis of the distribution and toxic effects of snPt is necessary.

Widespread application of sub-nanosized materials comes with an increased risk of human exposure and environmental release, and the future of nanotechnology will depend on the public acceptance of the risk-benefit ratio. The present study demonstrated that snPt induces hepatotoxicity *in vitro* and *in vivo*. However, our research also indicates that the toxicity of platinum particles could be reduced by altering their size. Additionally, biocompatible coatings can reduce the negative effects of nanoparticles on cells (Oberdorster et al. 2010; Nabeshi et al. 2011; Singh et al. 2007; Clift et al. 2008). Therefore, future studies will contribute to the development of sub-nanosized materials and will also help produce safer products.

4. Experimental

4.1. Materials

Platinum particles with a diameter of 15 nm (nPt) and less than 1 nm (snPt) were purchased from Polytech & Net GmbH (Rostock, Germany). The

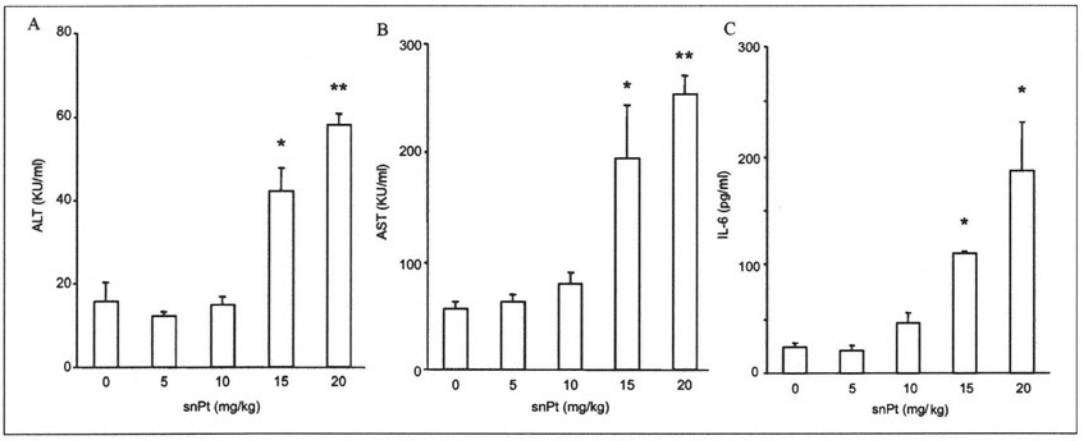

Fig. 2: Dose dependency of snPt-induced liver injury. snPt was intravenously administrated at 5, 10, 15 and 20 mg/kg. At 24 h after administration, blood was recovered, and the resultant serum was used for measurement of ALT (A), AST (B) and IL-6 (C), as described in the "Experimental" section. Data are means ± SEM (n = 3). *Significant difference when compared with the vehicle-treated group (*, $p < 0.05$, **, $p < 0.01$)

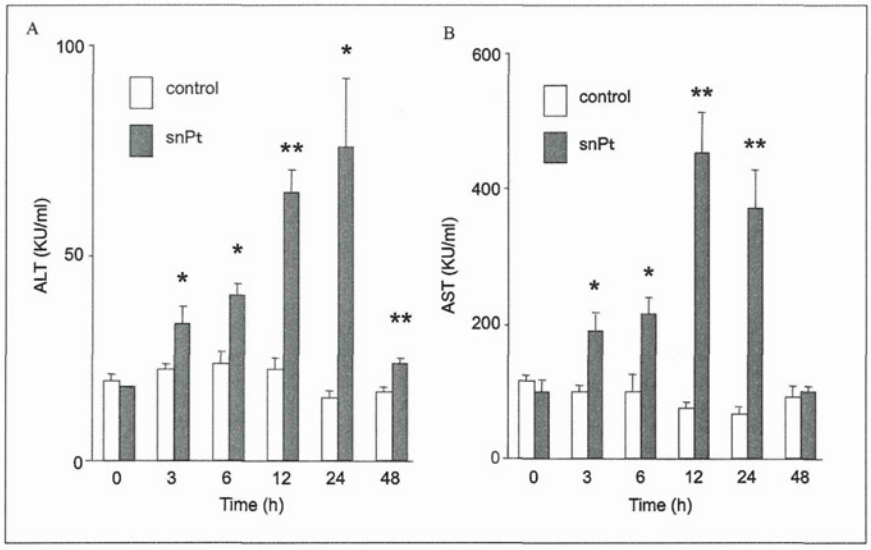

Fig. 3: Time-dependent changes of a biological marker of liver injury. snPt was intravenously administered to mice at 15 mg/kg. Blood was recovered at 3, 6, 12, 24 and 48 h after administration. The serum was used for measurement of ALT (A) and AST (B), as described in the "Experimental" section. Data are means ± SEM (n = 3). *Significant difference when compared with the vehicle-treated group (*, $p < 0.05$, **, $p < 0.01$)

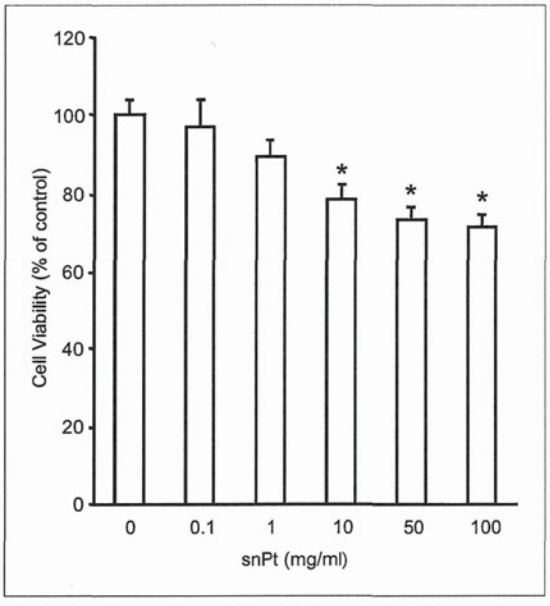

Fig. 4: Cytotoxicity of snPt in hepatic cells. Primary hepatocytes were treated with snPt at 0.1, 1, 10, 50 or 100 μg/ml. After 24 h of culture, cell viability was evaluated with the WST assay, as described in the "Experimental" section. Data are means ± SEM (n = 3). *Significant difference when compared with the vehicle-treated group ($P < 0.05$)

particles were stocked in a 5 mg/ml aqueous suspension. The stock solutions were suspended using a vortex mixer before use. Reagents used in this study were of research grade.

4.2. Animals

BALB/c male mice (8 weeks old) were obtained from Shimizu Laboratory Supplies Co., Ltd. (Kyoto, Japan), and were housed in an environmentally controlled room at 23 ± 1.5 °C with a 12 h light/12 h dark cycle. Mice had access to water and commercial chow (Type MF, Oriental Yeast, Tokyo, Japan). Mice were intravenously injected with nPt or snPt at 5 to 20 mg/kg body weight. The experimental protocols conformed to the ethical guidelines of the Graduate School of Pharmaceutical Sciences, Osaka University.

4.3. Cells

Mouse primary hepatocytes were isolated from BALB/c mice (Shimizu Laboratory Supplies Co.) by the collagenase-perfusion method (Seglen 1976). Isolated hepatocytes were suspended in Williams' E medium containing 10% fetal calf serum, 1 nM insulin, and 1 nM dexamethasone. Next, cell viability was assessed by Trypan blue dye exclusion. Cells that were at least 90% viable were used in this study. Cells were cultured in a humidified 5% CO_2 incubator at 37 °C.

4.4. Histological analysis

After intravenous administration of snPt, mouse livers were removed and fixed with 4% paraformaldehyde. Thin tissue sections were stained with hematoxylin and eosin for histological observation.

4.5. Biochemical assay

Serum alanine aminotransferase (ALT) and aspartate aminotransferase (AST) were measured using commercially available kits (WAKO Pure Chemical, Osaka, Japan), respectively. Interleukin-6 (IL-6) levels were measured with an ELISA kit (BioSource International, Camarillo, CA, USA). These assays were performed according to the manufacturer's protocols.

4.6. Cell viability assay

Cell viability was determined using WST-8 (Nacalai Tesque, Osaka, Japan), according to the manufacturer's protocol. Briefly, 1×10^4 cells/well were seeded on a 96 well plate at 37 °C overnight. After 24 h of treatment with snPt, WST-8 reagent was added to each well. The plate was incubated for 1 h at 37 °C and assessed at an absorbance of 450 nm by a plate reader. Obtained data were normalized to the control group, which was designated as 100%.

4.7. Statistical analysis

Data are presented as means ± SD. Statistical analysis was performed by student's t-test. $P < 0.05$ was considered statistically significant.